Journal of Nonlinear Modeling and Analysis
Volume 7, Number 6, December 2025, 2013–2047
https://journal.global-sci.org/jnma
DOI:10.12150/jnma.2025.2013

Numerical Approximation of the System of Fractional Differential Equations Using the Fibonacci Wavelet Collocation Method

Manohara G[1] and Kumbinarasaiah S[2,†]

Abstract This study uses the Fibonacci wavelet collocation method (FWCM) to solve the system of fractional differential equations. Here, we introduce the innovative Fibonacci wavelet method with the help of an operational matrix of integration generated by the Fibonacci polynomials to compute the approximate solution of the linear and nonlinear fractional differential equations. The Fibonacci wavelet collocation method, initially developed for a system of differential equations of integer order, can approximate the solutions to systems of fractional differential equations of fractional order. This method converts the system of fractional differential equations into a system of algebraic equations. These algebraic equations are then solved using the Newton-Raphson method, and the estimated values of the coefficients are then substituted in the approximation. Numerical outcomes are obtained to illustrate the simplicity and effectiveness of the proposed scheme. The numerical results demonstrate that the method is simple to use and precise. The effectiveness and consistency of the developed strategy's performance are shown in graphs and tables. The method introduces a potential technique for resolving several linear and nonlinear fractional differential equations. Mathematical software called Mathematica has been used to perform all calculations.

Keywords Fractional differential equations (FDEs), collocation technique, Riemann-Liouville fractional derivative, Fibonacci wavelet

MSC(2010) 34B16, 34A12, 6L05, 65L10.

1. Introduction

Differential equations with arbitrary (fractional) order derivatives are called fractional differential equations (FDEs). Improved rheological models are the foundation for mathematical modelling that naturally produces FDEs. This idea generalizes the classical differential equations. Many works have been published where fractional derivatives describe better material properties, particularly in hereditary solid mechanics and viscoelasticity theory. FDEs are receiving much attention because of their frequent appearance in several applications in signal processing, biology, physics, acoustics, robotics, fluid mechanics, viscoelasticity, and engineering. Determining the exact solutions to physical phenomena is crucial to understanding

[†]the corresponding author.
Email address: kumbinarasaiah@bub.ernet.in; kumbinarasaiah@gmail.com
[1]Department of Mathematics and Statistics, Ramaiah University of Applied Sciences, Bengaluru-560058, India
[2]Department of Mathematics, Bangalore University, Bengaluru-560056, India

and applying them in scientific research.

To analytically approximate the nonlinear FDEs, a few semi-analytical methods have been proposed, including the ADM [2], the HAM [3], the Homotopy asymptotic method [4], the multistep fractional differential transform method (MFDTM) [5], and the HPM [6]. Unfortunately, these techniques have limitations and cannot provide the high-precision solution of complex FDEs in many situations, especially in the unbounded domain. Therefore, there is no doubt that numerical approaches are superior to analytical ones. Since most FDEs lack precise analytical solutions, numerical techniques are frequently used. A significant area of current research has been the development of accurate and capable methods for solving FDEs. However, despite many recently formulated applied problems, the state of the art is far less advanced for generalized order equations, and only a few techniques have been proposed for numerically solving these equations. Most of these numerical schemes deal with linear single-term equations of order smaller than unity. Little efforts have been made to address nonlinear problems. Few numerical approaches have been put forward to address the system of nonlinear FDEs: the ADM method [7], the DTM method [8], the HPM method [9], the Bernoulli wavelet method (BWM) [10], and the Legendre wavelet method (LWM) [11].

Consider the SODEs is of the form:

$$\left.\begin{aligned} D^{\alpha_1}\ y_1(\xi) &= f_1(\xi, y_1, y_2, \ldots, y_n),\\ D^{\alpha_2}\ y_2(\xi) &= f_2(\xi, y_1, y_2, \ldots, y_n),\\ &\vdots\\ D^{\alpha_n}\ y_n(\xi) &= f_n(\xi, y_1, y_2, \ldots, y_n), \end{aligned}\right\} \tag{1.1}$$

where D^{α_i} is the derivative of y_i of order α_i in the sense of Riemann-Liouville fractional derivative and $0 \leq \alpha_i \leq 1$, concerning the primary constraints $y_1(0) = d_1,\ y_2(0) = d_2,\ \ldots,\ y_n(0) = d_n$.

Wavelets are among the many data types that can extract information mathematically. Sets of wavelets are necessary for the complete investigation of data. Wavelets allow reversible signal decomposition by mathematically breaking it into smaller pieces without overlaps or gaps. Sets of wavelets are valuable in wavelet-based compression/decompression techniques because retrieving the original information with little loss is desirable. Over the past 20 years, wavelet theory has been used in various signal processing applications, such as fingerprint verification, wavelet-based fingerprint storage, denoising of data, musical tone generation, etc. [12]. The orthogonal, compactly supported wavelet basis precisely approximates an increasingly higher-order polynomial. This wavelet-based representation of differential operations can be precise and stable even in areas with significant gradients or oscillations. For some of the standard mathematical problems, various wavelet collocation techniques have been used, such as the Chebyshev wavelet collocation method [13, 14], collocation method based on Bernoulli and Gegenbauer wavelets [15], Hermite wavelet collocation method [16], and Laguerre wavelet collocation method [17, 46]. Several wavelet collocation techniques are typically employed to solve fractional differential equations, which include Chelyshkov wavelets [18], Cubic B Spline [19], Genocchi wavelets [20], Taylor wavelets [21, 22], Haar wavelets [23], Bernoulli wavelets [10, 24], Hermite wavelets [25, 26], Legendre wavelets and Legendre wavelet tau method [27–29], Chebyshev wavelets [30], Gegenbaur wavelets [31] and Ultraspherical wavelets [32].

The Fibonacci wavelet collocation method is an interesting approach that combines ideas from wavelet theory and numerical methods to solve differential equations. Combining wavelets with the collocation method means using wavelet basis functions to approximate the solution of the differential equation. This method offers several advantages:
Locality and Efficiency: Wavelets are localized, so they can represent functions efficiently in regions where the function has significant features, leading to potentially faster computations and more accurate solutions.
Flexibility: Using wavelets allows for adaptive resolution, where finer resolution (more detail) can be used in regions where the solution changes rapidly and coarser resolution elsewhere.
Numerical Stability: Wavelets can help improve the stability and convergence properties of the numerical method, especially for complex or irregular problems.

It has an added advantage in contrast with the other wavelet methods as follows:

- The number of terms of the Fibonacci polynomials $P_m(\xi)$ is less than the number of the terms of the Legendre polynomials $L_m(\xi)$. It helps to reduce the CPU time.
- Error components in the operational matrix of integration representing Fibonacci polynomials are less than those of Legendre polynomials.
- Fibonacci polynomials $P_m(\xi)$ have smaller coefficients of individual terms than the corresponding ones in Legendre polynomials $L_m(\xi)$. Computational errors can be reduced using this property.
- The coefficient of individual terms in Fibonacci polynomials $P_m(\xi)$, are smaller than the corresponding ones in Legendre polynomials $L_m(\xi)$. As a result, using Fibonacci polynomials reduces computational errors.
- Fibonacci wavelets are superior to those not based on orthogonal polynomials, but we can express the Fibonacci polynomials as approximate orthogonal polynomials.
- Using the Mathematica command $Fibonacci[m, \xi]$, the coefficients of the Fibonacci polynomials can be easily obtained in computer programs.

The Fibonacci wavelet method suits solutions with sharp edge/jump discontinuities. By making slight modifications to the method,

- The Fibonacci wavelet method can solve the higher-order system of ordinary differential equations.
- This method can be extended to PDEs and other mathematical models with different physical conditions.
- It is used to obtain the solution of the differential equation in the universal domain by taking the suitable transformation.
- Fractional differential equations, delay differential equations and stiff systems can be solved using this method directly without using any control parameters.

Here, the Fibonacci wavelet collocation technique was successfully applied to the model, and significant approximation was obtained in the model's solution. To our knowledge, no one has solved this system of FDEs by Fibonacci wavelets,

which motivates us to study this using the developed strategy. The absolute error with the exact solution and ND Solver solution for various values of M and k is computed to demonstrate the efficacy and accuracy of the developed strategy. Developing a quick and easy FWCM is the goal of the current effort. It ensures that the SFDEs can be solved with sufficient precision for just a few grid points. Utilizing a novel numerical design makes it difficult to determine the necessary approximations. Researchers have used this package to solve mathematical problems such as fractional order Brusselator chemical model [33], time-fractional telegraph equation [34], dual-phase-lag heat transfer model [35], time-varying delay problems [36], Emden-Fowler equations [37], nonlinear reaction-diffusion equations of Fisher type [38], time-fractional bioheat transfer model [39], hyperbolic partial differential equation [1], nonlinear Volterra integral equation [40], biological models [41], spectral solution of FDEs [42], nonlinear Hunter-Saxton equation [43], and nonlinear stratonovich Volterra integral equations [44].

Here is how the article is structured. The wavelets are defined in Section 2, "Preliminaries". Section 3 involves the OMI of Fibonacci wavelets. Sections 4 and 5 explain the problem's process and use of the suggested methodology. The article's conclusion is provided in Section 6.

2. Preliminaries of the Fibonacci wavelets

Definition 2.1. Riemann-Liouville fractional derivative:

The Riemann-Liouville integral operator of order α is defined by [40]:

$$\left(I^{\alpha}u\right)(\xi)=\begin{cases}\frac{1}{\Gamma(\alpha)}\int_0^{\xi}(\xi-t)\,u(t)\,dt, & \alpha>0,\ t>0,\\ u(t), & \alpha=0.\end{cases}$$

Its fractional derivative order α $(\alpha \geq 0)$ is normally used:

$$\left(D^{\alpha}u\right)(\xi)=\left(\frac{d}{dt}\right)^{n}\ (I^{n-\alpha}\ u)(\xi),\quad \alpha>0,\quad n-1<\alpha\ \leq n.$$

Definition 2.2. Fibonacci wavelets:

The mother wavelets dilate and translate themselves to build a family of functions. We coin the term wavelets to describe them. The family's wavelets are as follows: [36]

$$\vartheta_{p,q}(\xi)=|p|^{-\frac{1}{2}}\ \vartheta\left(\frac{\xi-q}{-p}\right),\quad p,q\in\mathbb{R},\ p\ \neq 0.$$

The dilation and translation parameters are indicated by the letters p and q, respectively. Furthermore, q varies continuously. If we choose $p=p_0^{-k}$, $q=np_0^{-k}q_0$, $p_0>1$, $q_0>1$, and n and k are positive integers, the discrete wavelet family is introduced as,

$$\vartheta_{k,n}(\xi)=|p_0|^{\frac{k}{2}}\quad \vartheta\left(p_0^{k}\xi-nq_0\right),$$

where $\vartheta_{k,n}(\xi)$ is the wavelet basis in $L^2(\mathbb{R})$.

Fibonacci wavelets $\vartheta_{n,m}(\xi)=\vartheta(k\ ,\hat{n},m\ ,\xi)$ have four parameters; $\hat{n}=n-1, n=1,2,3,\ldots,2^{k-1}$, k is a positive integer, m is the degree of Fibonacci polynomials, and ξ is the normalized time. On the interval [0,1], the Fibonacci wavelets

are defined as [34, 45],

$$\vartheta_{n,m}(\xi) = \begin{cases} \frac{2^{\frac{k-1}{2}}}{\sqrt{w_m}} P_m(2^{k-1}\xi - \widehat{n}), & \frac{\widehat{n}}{2^{k-1}} \leq \xi < \frac{\widehat{n}+1}{2^{k-1}}, \\ 0, & \text{otherwise}, \end{cases}$$

with

$$w_m = \int_0^1 (P_m(\xi))^2 d\xi,$$

where $P_m(\xi)$ is the Fibonacci polynomial of degree $m = 0, 1, ..., M-1$, translation parameter $n = 1, 2, ..., 2^{k-1}$ and k represents the level of resolution $k = 1, 2, ...$, respectively. The quantity $\frac{1}{\sqrt{w}_m}$ is a normalization factor. The Fibonacci polynomials are defined as follows in the form of the recurrence relation for every $\xi \in R^+$,

$$P_{m+2}(\xi) = \xi P_{m+1}(\xi) + P_m(\xi), \ \forall m \geq 0,$$

subject to primary constraints $P_0(\xi) = 1, \ P_1(\xi) = \xi$. Additionally, these polynomials can be defined with the following universal formula:

$$P_m(\xi) = \begin{cases} 1, & m = 0, \\ \xi, & m = 1, \\ \xi P_{m-1}(\xi) + P_{m-2}(\xi), & m > 1. \end{cases}$$

Furthermore, these polynomials can be represented in the power form as follows:

$$P_m(\xi) = \sum_{i=0}^{\lfloor \frac{m}{2} \rfloor} \binom{m-i}{i} \xi^{m-2i}, \quad m > 0.$$

If $P_m(\xi), m = 0, 1, 2, \ldots, M-1$ are the Fibonacci polynomials, then [36],

$$\int_0^1 P_m(\xi) \ P_n(\xi) = \sum_{i=0}^{\lfloor \frac{m}{2} \rfloor} \sum_{j=0}^{\lfloor \frac{m}{2} \rfloor} \binom{m-i}{i} \binom{n-j}{j} \frac{1}{m+n-2i-2j+1}.$$

Fibonacci wavelets are compactly supported wavelets formed by Fibonacci polynomials over the interval [0,1].

Theorem 2.1. *[33] Let $L^2[0,1]$ be the Hilbert space generated by the Fibonacci wavelet basis. Let $\eta(\xi)$ be the continuous bounded function in $L^2[0,1]$. Then, the Fibonacci wavelet expansion of $\eta(\xi)$ converges with it.*

Proof. Let $\eta : [0,1] \longrightarrow \mathbb{R}$ be a continuous function and $|\eta(\xi)| \leq \varsigma$, where ς is any real number. Then, the Fibonacci wavelet dilation of $\eta(\xi)$ can be expressed as

$$\eta(\xi) = \sum_{n=1}^{2^{\frac{k-1}{2}}} \sum_{m=0}^{M-1} a_{n,m} \ \vartheta_{n,m}(\xi),$$

where $a_{n,m} = \langle \ \eta(\ \xi\ ), \ \vartheta_{n,m}(\xi) \rangle$ denotes inner product.

$$a_{n,m} = \int_0^1 \eta(\xi) \ \vartheta_{n,m}(\xi) \, d\xi.$$

$a_{n,m} = \int_I \eta\ (\xi)\ \frac{2^{\frac{k-1}{2}}}{\sqrt{Z_m}}\ P_m\left(2^{k-1}\xi - n + \ 1\right)\ d\xi$ where $I = \left[\frac{n}{2^{k-1}} - 1\ ,\ \ \frac{n}{2^{k-1}}\right)$.

Then, substituting $2^{k-1}\xi - n + 1 = y$ then, we get,

$$a_{n,m} = \frac{2^{\frac{k-1}{2}}}{\sqrt{Z_m}} \int_0^1 \eta\left(\frac{y\ +\ n-1}{2^{k-1}}\right) P_m\left(y\right) \frac{dy}{2^{k-1}}.$$

By generalized mean value theorem,

$$a_{n,m}\ = \frac{2^{\frac{1-k}{2}}}{\sqrt{Z_m}} \eta\left(\frac{\zeta + n - 1}{2^{\ k-\ 1}}\right) \int_0^1 P_m(\ y\ ) dy \quad \text{for some} \quad \zeta \in (0,1).$$

Since $P_m(y)$ is a bounded continuous function, put $\int_0^1 P_m(y)dy = h$,

$$|a_{n,m}|\ = \left|\frac{2^{\frac{-k+1}{2}}}{\sqrt{Z_m}}\right| \left|\eta\left(\frac{\zeta + n - \ 1}{2^{k-1}}\right)\right| h\ .$$

Since η remains bounded,

$$|a_{n,m}|\ = \left|\frac{2^{\ \frac{-k+1}{2}} \varsigma h}{\sqrt{Z_m}}\right|.$$

Therefore, $\sum_{n,m=0}^{\infty} a_{n,m}$ is absolutely convergent. Hence, the Fibonacci wavelet series expansion $\eta(\xi)$ converges uniformly to it. □

Remark 2.1. Error estimation for continuous bounded function $\eta(\xi)$ using the above Theorem 2.1. $\eta(\xi)$ is the exact solution and $\eta_{app}(\xi)$ is the Fibonacci wavelet approximation, where

$$\eta(\xi) = \sum_{n=1}^{\infty} \sum_{m=0}^{\infty} a_{n,m} \vartheta_{n,m}(\xi),$$

$$\eta_{\text{app}}(\xi) = \sum_{n=1}^{2^{\frac{k-1}{2}}} \sum_{m=0}^{M-1} a_{n,m} \vartheta_{n,m}(\xi),$$

$$\eta(\xi) - \eta_{\text{app}}(\xi) = \sum_{n=1}^{\infty} \sum_{m=0}^{\infty} a_{n,m} \vartheta_{n,m}(\xi) - \sum_{n=1}^{2^{\frac{k-1}{2}}} \sum_{m=0}^{M-1} a_{n,m} \vartheta_{n,m}(\xi)$$

$$= \sum_{n=2^k}^{\infty} \sum_{m=M}^{\infty} a_{n,m} \vartheta_{n,m}(\xi).$$

Now,

$$\|E_n\|^2 = \|\eta\ (\xi) - \eta_{app}\,(\xi)\|^2 = \langle \eta\ (\xi) - \eta_{app}\,(\xi)\,,\, \eta\ (\xi) - \eta_{app}\,(\xi)\rangle\,,$$

$$\Longrightarrow \|E_n\|^2 = \int_0^1 \sum_{n=2^k}^{\infty} \sum_{m=M}^{\infty} a_{n,m}^2\ \vartheta_{n,m}^2\ (\xi).$$

But from the above theorem, we have,

$$|a_{n,m}|\ \leq \left|\frac{2^{\ \frac{-k+1}{2}}}{\sqrt{Z_m}}\ \varsigma\ h\right|\ ,$$

$$\Longrightarrow \|E_n\|^2 \leq \int_0^1 \sum_{n=2^k}^{\infty} \sum_{m=M}^{\infty} \frac{2^{-k+1}}{Z_m}\ \mu^2\ h^2 \vartheta_{n,m}^2\ (\xi).$$

Theorem 2.2. *[33] Let $I \subset R$ be a finite interval with length $m(I)$. Furthermore, $f(\xi)$ is an integrable function defined on I and let $\sum_{i=0}^{M-1} \sum_{j=1}^{2^{k-1}} a_{i,j}\ \vartheta_{i,j}(\xi)$ be a good Fibonacci wavelet approximation of f on I with satisfying for some $\epsilon\ > 0$, $\left| f\,(\xi) - \sum_{i=0}^{M-1} \sum_{j=1}^{2^{k-1}} a_{i,j} \vartheta_{i,j}(\xi) \right| \leq \epsilon, \quad \forall\ x\ \in I.$*
Then,
$-\epsilon\ m\,(I) + \int_I \sum \sum\ a_{i,j}\ \vartheta_{i,j}(\xi)\ d\xi\ \leq \int_I f\,(\xi)\, d\xi\ \leq\ \epsilon\ m\,(I) + \int_I \sum \sum\ a_{i,j}\ \vartheta_{i,j}(\xi)\ d\xi.$

3. Operational matrix of integration (OMI)

The author of [1] created the Fibonacci wavelet basis at $k = 1$ and $M = 6$, from which the functional matrix was derived as follows:

$$\begin{aligned}
\vartheta_{1,0}(\xi) =& 1,\\
\vartheta_{1,1}(\xi) =& \sqrt{3\xi},\\
\vartheta_{1,2}(\xi) =& \frac{1}{2}\sqrt{\frac{15}{7}}(1+\xi^2),\\
\vartheta_{1,3}(\xi) =& \sqrt{\frac{105}{239}}\,\xi\,(2+\xi^2),\\
\vartheta_{1,4}(\xi) =& 3\sqrt{\frac{35}{1943}}\,(1+3\xi^2+\xi^4),\\
\vartheta_{1,5}(\xi) =& \frac{3}{4}\sqrt{\frac{385}{2582}}\,\xi\,(3+4\xi^2+\xi^4),\\
\vartheta_{1,6}(\xi) =& 3\sqrt{\frac{5005}{1268209}}\,(1+6\xi^2+5\xi^4+\xi^6),\\
\vartheta_{1,7}(\xi) =& 3\sqrt{\frac{5005}{2827883}}\,\xi\,(4+10\xi^2+15\xi^4+7\xi^6+\xi^8).
\end{aligned}$$

After integrating the first six bases mentioned above regarding the limit ξ between 0 and ξ, and expressing the Fibonacci wavelet bases as a linear combination, we obtain

$$\int_0^{\xi} \vartheta_{1,0}(\xi)d\xi = \begin{bmatrix} 0 & \frac{1}{\sqrt{3}} & 0 & 0 & 0 & 0 \end{bmatrix} \vartheta_6(\xi),$$

$$\int_0^{\xi} \vartheta_{1,1}(\xi)d\xi = \begin{bmatrix} -\frac{\sqrt{3}}{2} & 0 & \sqrt{\frac{7}{5}} & 0 & 0 & 0 \end{bmatrix} \vartheta_6(\xi),$$

$$\int_0^{\xi} \vartheta_{1,2}(\xi)d\xi = \begin{bmatrix} 0 & \frac{\sqrt{5}}{6\sqrt{7}} & 0 & \frac{\sqrt{239}}{42} & 0 & 0 \end{bmatrix} \vartheta_6(\xi),$$

$$\int_0^{\xi} \vartheta_{1,3}(\xi)d\xi = \begin{bmatrix} -\frac{\sqrt{105}}{2\sqrt{239}} & 0 & \frac{7}{2\sqrt{239}} & 0 & \frac{\sqrt{1943}}{4\sqrt{717}} & 0 \end{bmatrix} \vartheta_6(\xi),$$

$$\int_0^{\xi} \vartheta_{1,4}(\xi)d\xi = \left[0 \quad 0 \quad 0 \quad \frac{\sqrt{717}}{5\sqrt{1943}} \quad 0 \quad \frac{4\sqrt{2582}}{5\sqrt{21373}}\right]\vartheta_6(\xi),$$

$$\int_0^{\xi} \vartheta_{1,5}(\xi)d\xi = \left[-\frac{\sqrt{385}}{4\sqrt{2582}} \quad 0 \quad 0 \quad 0 \quad \frac{\sqrt{21373}}{24\sqrt{2582}} \quad 0\right]\vartheta_6(\xi),$$

$$\int_0^{\xi} \vartheta\left(\xi\right)d\xi = \mathcal{B}_{6\times 6}\ \vartheta_6\left(\xi\right) + \overline{\vartheta_6(\xi)}, \tag{3.1}$$

where

$$\vartheta_6(x) = [\vartheta_{1,0}(\xi), \vartheta_{1,1}(\xi), \vartheta_{1,2}(\xi), \vartheta_{1,3}(\xi), \vartheta_{1,4}(\xi), \vartheta_{1,5}(\xi)]^T,$$

$$\mathcal{B}_{6\times 6} = \begin{bmatrix} 0 & \frac{1}{\sqrt{3}} & 0 & 0 & 0 & 0 \\ -\frac{\sqrt{3}}{2} & 0 & \sqrt{\frac{7}{5}} & 0 & 0 & 0 \\ 0 & \frac{\sqrt{5}}{6\sqrt{7}} & 0 & \frac{\sqrt{239}}{42} & 0 & 0 \\ -\frac{\sqrt{105}}{2\sqrt{239}} & 0 & \frac{7}{2\sqrt{239}} & 0 & \frac{\sqrt{1943}}{4\sqrt{717}} & 0 \\ 0 & 0 & 0 & \frac{\sqrt{717}}{5\sqrt{1943}} & 0 & \frac{4\sqrt{2582}}{5\sqrt{21373}} \\ -\frac{\sqrt{385}}{4\sqrt{2582}} & 0 & 0 & 0 & \frac{\sqrt{21373}}{24\sqrt{2582}} & 0 \end{bmatrix},$$

$$\overline{\vartheta_6(\xi)} = \begin{bmatrix} 0 \\ 0 \\ 0 \\ 0 \\ 0 \\ \frac{\sqrt{1268209}}{24\sqrt{33566}}\vartheta_{1,6}(\xi) \end{bmatrix}.$$

Integrating the previously mentioned bases once again yields the following results:

$$\int_0^{\xi}\int_0^{\xi} \vartheta_{1,0}(\xi)d\xi d\xi = \left[\frac{1}{2} \quad 0 \quad \sqrt{\frac{7}{15}} \quad 0 \quad 0 \quad 0\right]\vartheta_6(\xi),$$

$$\int_0^{\xi}\int_0^{\xi} \vartheta_{1,1}(\xi)d\xi d\xi = \left[0 \quad -\frac{1}{3} \quad 0 \quad \frac{\sqrt{239}}{6\sqrt{35}} \quad 0 \quad 0\right]\vartheta_6(\xi),$$

$$\int_0^{\xi}\int_0^{\xi} \vartheta_{1,2}(\xi)d\xi d\xi = \left[-\frac{\sqrt{5}}{2\sqrt{21}} \quad 0 \quad \frac{1}{4} \quad 0 \quad \frac{\sqrt{1943}}{168\sqrt{3}} \quad 0\right]\vartheta_6(\xi),$$

$$\int_0^{\xi}\int_0^{\xi} \vartheta_{1,3}(\xi)d\xi d\xi = \left[0 \quad -\frac{5\sqrt{35}}{12\sqrt{239}} \quad 0 \quad \frac{2}{15} \quad 0 \quad \frac{\sqrt{2582}}{5\sqrt{7887}}\right]\vartheta_6(\xi),$$

$$\int_0^\xi \int_0^\xi \vartheta_{1,4}(\xi)d\xi d\xi = \left[-\frac{\sqrt{35}}{2\sqrt{1943}} \quad 0 \quad \frac{7\sqrt{3}}{10\sqrt{1943}} \quad 0 \quad \frac{1}{12} 0 \quad \right] \vartheta_6(\xi),$$

$$\int_0^\xi \int_0^\xi \vartheta_{1,5}(\xi)d\xi d\xi = \left[0 \quad -\frac{\sqrt{385}}{4\sqrt{7746}} \quad 0 \quad \frac{\sqrt{2629}}{40\sqrt{7746}} \quad 0 \quad \frac{2}{35} \right] \vartheta_6(\xi).$$

Hence,

$$\int_0^\xi \int_0^\xi \vartheta(\xi)d\xi d\xi = \mathcal{B}_{6\times 6}^{'} \ \vartheta_6(\xi) + \overline{\vartheta_6^{'}(\xi)}. \tag{3.2}$$

$$\mathcal{B}_{6\times 6}^{\prime} = \begin{bmatrix} -\frac{1}{2} & 0 & \sqrt{\frac{7}{15}} & 0 & 0 & 0 \\ 0 & -\frac{1}{3} & 0 & \frac{\sqrt{239}}{6\sqrt{35}} & 0 & 0 \\ -\frac{\sqrt{5}}{2\sqrt{21}} & 0 & \frac{1}{4} & 0 & \frac{\sqrt{1943}}{168\sqrt{3}} & 0 \\ 0 & -\frac{5\sqrt{35}}{12\sqrt{239}} & 0 & \frac{2}{15} & 0 & \frac{\sqrt{2582}}{5\sqrt{7887}} \\ -\frac{\sqrt{35}}{2\sqrt{1943}} & 0 & \frac{7\sqrt{3}}{10\sqrt{1943}} & 0 & \frac{1}{12} & 0 \\ 0 & -\frac{\sqrt{385}}{4\sqrt{7746}} & 0 & \frac{\sqrt{2629}}{40\sqrt{7746}} & 0 & \frac{2}{35} \end{bmatrix},$$

$$\overline{\vartheta_6^{'}(\xi)} = \begin{bmatrix} 0 \\ 0 \\ 0 \\ 0 \\ \frac{\sqrt{1268209}}{30\sqrt{277849}}\vartheta_{1,6}(\xi) \\ \frac{\sqrt{2827883}}{168\sqrt{33566}}\vartheta_{1,7}(\xi) \end{bmatrix}.$$

Similarly, the third integration can be expressed as

$$\int_0^\xi \int_0^\xi \int_0^\xi \vartheta\left(\xi\right) d\xi = = \mathcal{B}_{6\times 6}^{''} \ \vartheta_6(\xi) + \overline{\vartheta_6^{''}(\xi)}, \tag{3.3}$$

where

$$\mathcal{B}_{6\times 6}^{\prime\prime} = \begin{bmatrix} 0 & -\frac{1}{3\sqrt{3}} & 0 & \frac{\sqrt{239}}{6\sqrt{35}} & 0 & 0 \\ \frac{1}{4\sqrt{3}} & 0 & -\frac{\sqrt{7}}{4\sqrt{5}} & 0 & \frac{\sqrt{1943}}{24\sqrt{105}} & 0 \\ 0 & -\frac{\sqrt{5}}{8\sqrt{7}} & 0 & \frac{\sqrt{239}}{140} & 0 & \frac{\sqrt{1291}}{105\sqrt{66}} \\ \frac{\sqrt{105}}{8\sqrt{239}} & 0 & -\frac{49}{20\sqrt{239}} & 0 & \frac{\sqrt{1943}}{24\sqrt{717}} & 0 \\ 0 & -\frac{3\sqrt{21}}{4\sqrt{9715}} & 0 & \frac{\sqrt{239}}{10\sqrt{5829}} & 0 & \frac{3\sqrt{2582}}{35\sqrt{21373}} \\ \frac{3\sqrt{385}}{32\sqrt{2582}} & 0 & -\frac{133\sqrt{11}}{80\sqrt{7746}} & 0 & \frac{\sqrt{21373}}{224\sqrt{2582}} & 0 \end{bmatrix}$$

and

$$\overline{\vartheta_6^{'}(\xi)} = \begin{bmatrix} 0 \\ 0 \\ 0 \\ \frac{\sqrt{\frac{1268209}{277849}}}{30}\vartheta_{1,6}\left(\xi\right) \\ \frac{\sqrt{\frac{2827883}{33566}}}{168}\vartheta_{1,7}\left(\xi\right) \\ \frac{\sqrt{11941544471}}{360\sqrt{5016284989}}\vartheta_{1,6}\left(\xi\right) + \frac{\sqrt{7939564237061}}{1320\sqrt{576872773735}}\vartheta_{1,8}\left(\xi\right) \end{bmatrix}.$$

At $k = 2$ and $M = 6$, the FWB is investigated as follows:

$$\left.\begin{aligned} \vartheta_{1,0}\left(\xi\right) &= \sqrt{2}, \\ \vartheta_{1,1}\left(\xi\right) &= 2\sqrt{6}\xi, \\ \vartheta_{1,2}\left(\xi\right) &= \sqrt{\tfrac{15}{14}}\left(1 + 4\xi^2\right), \\ \vartheta_{1,3}\left(\xi\right) &= 4\sqrt{\tfrac{210}{239}}\left(\xi + 2\xi^3\right), \\ \vartheta_{1,4}\left(\xi\right) &= 3\sqrt{\tfrac{70}{1943}}\left(1 + 12\xi^2 + 16\xi^4\right), \\ \vartheta_{1,5}\left(\xi\right) &= \tfrac{3}{2}\sqrt{\tfrac{385}{1291}}\xi\left(3 + 16\xi^2 + 16\xi^4\right), \end{aligned}\right\} \quad 0 \leq \xi < \frac{1}{2}.$$

$$\left.\begin{aligned}
&\vartheta_{2,0}(\xi)=\sqrt{2},\\
&\vartheta_{2,1}(\xi)=\sqrt{6}\,(-1+2\xi),\\
&\vartheta_{2,2}(\xi)=\sqrt{\tfrac{30}{7}}\left(1-2\xi+2\xi^2\right),\\
&\vartheta_{2,3}(\xi)=\sqrt{\tfrac{210}{239}}\,(-1+2\xi)\left(3-4\xi+4\xi^2\right),\\
&\vartheta_{2,4}(\xi)=3\sqrt{\tfrac{70}{1943}}\left(5-20\xi+36\xi^2-32\xi^3+16\xi^4\right),\\
&\vartheta_{2,5}(\xi)=6\sqrt{\tfrac{385}{1291}}\,(-1+2\xi)\left(1-3\xi+5\xi^2-4\xi^3+2\xi^4\right),
\end{aligned}\right\}\qquad \frac{1}{2}\le\xi<1.$$

$$\int_0^{\xi}\vartheta(\xi\ )\ d\xi=\mathcal{B}_{12\times12}\ \vartheta_{12}(\xi)+\overline{\vartheta_{12}(\xi)},\tag{3.4}$$

where

$$\vartheta_{12}(\xi)=[\vartheta_{1,0}(\xi),\ \vartheta_{1,1}(\xi),\vartheta_{1,2}(\xi),\vartheta_{1,3}(\xi),\ \vartheta_{1,4}(\xi),\vartheta_{1,5}(\xi),\ \vartheta_{2,0}(\xi),\vartheta_{2,1}(\xi),\ \vartheta_{2,2}(\xi),\vartheta_{2,3}(\xi),\vartheta_{2,4}(\xi),\vartheta_{2,5}(\xi)]^T,$$

$$\mathcal{B}_{12\times12}=\begin{bmatrix}
0 & \frac{1}{2\sqrt{3}} & 0 & 0 & 0 & 0 & 0 & 0 & 0 & 0 & 0 & 0\\
-\frac{\sqrt{3}}{4} & 0 & \frac{\sqrt{\frac{7}{5}}}{2} & 0 & 0 & 0 & 0 & 0 & 0 & 0 & 0 & 0\\
0 & \frac{\sqrt{5}}{12\sqrt{7}} & 0 & \frac{\sqrt{239}}{84} & 0 & 0 & 0 & 0 & 0 & 0 & 0 & 0\\
-\frac{\sqrt{105}}{4\sqrt{239}} & 0 & \frac{7}{4\sqrt{239}} & 0 & \frac{\sqrt{1943}}{8\sqrt{717}} & 0 & 0 & 0 & 0 & 0 & 0 & 0\\
0 & 0 & 0 & \frac{\sqrt{717}}{10\sqrt{1943}} & 0 & \frac{2\sqrt{2582}}{5\sqrt{21373}} & 0 & 0 & 0 & 0 & 0 & 0\\
-\frac{\sqrt{385}}{8\sqrt{2582}} & 0 & 0 & 0 & \frac{\sqrt{21373}}{48\sqrt{2582}} & 0 & 0 & 0 & 0 & 0 & 0 & 0\\
0 & 0 & 0 & 0 & 0 & 0 & 0 & \frac{1}{2\sqrt{3}} & 0 & 0 & 0 & 0\\
0 & 0 & 0 & 0 & 0 & 0 & -\frac{\sqrt{3}}{4} & 0 & \frac{\sqrt{\frac{7}{5}}}{2} & 0 & 0 & 0\\
0 & 0 & 0 & 0 & 0 & 0 & 0 & \frac{\sqrt{5}}{12\sqrt{7}} & 0 & \frac{\sqrt{239}}{84} & 0 & 0\\
0 & 0 & 0 & 0 & 0 & 0 & -\frac{\sqrt{105}}{4\sqrt{239}} & 0 & 0 & 0 & \frac{\sqrt{21373}}{48\sqrt{2582}} & 0\\
0 & 0 & 0 & 0 & 0 & 0 & 0 & 0 & 0 & \frac{\sqrt{717}}{10\sqrt{1943}} & 0 & \frac{2\sqrt{2582}}{5\sqrt{21373}}\\
0 & 0 & 0 & 0 & 0 & 0 & -\frac{\sqrt{385}}{8\sqrt{2582}} & 0 & 0 & 0 & \frac{\sqrt{21373}}{48\sqrt{2582}} & 0
\end{bmatrix}$$

and

$$\overline{\vartheta_{12}}\left(\xi\right)=\begin{bmatrix}0\\0\\0\\0\\0\\\frac{\sqrt{\frac{1268209}{33566}}}{48}\vartheta_{1,6}\left(\xi\right)\\0\\0\\0\\0\\0\\\frac{\sqrt{\frac{1268209}{33566}}}{48}\vartheta_{2,6}\left(\xi\right)\end{bmatrix}.$$

Similar to the first integration, the second integration can be expressed as:

$$\int_0^\xi\int_0^\xi\vartheta(\xi)d\xi d\xi=\mathcal{B}_{12\times12}^{'}\ \vartheta_{12}(\xi)+\overline{\vartheta_{12}^{'}(\xi)},\tag{3.5}$$

where

$$\vartheta_{12}\left(\xi\right)=[\vartheta_{1,0}\left(\xi\right),\ \vartheta_{1,1}\left(\xi\right),\vartheta_{1,2}\left(\xi\right),\vartheta_{1,3}\left(\xi\right),\ \vartheta_{1,4}\left(\xi\right),\vartheta_{1,5}\left(\xi\right),\ \vartheta_{2,0}\left(\xi\right),\vartheta_{2,1}\left(\xi\right),\\ \vartheta_{2,2}\left(\xi\right),\vartheta_{2,3}\left(\xi\right),\vartheta_{2,4}\left(\xi\right),\vartheta_{2,5}\left(\xi\right)]^T,$$

$$\mathcal{B}'_{12\times12}=\begin{bmatrix}-\frac{1}{8}&0&\frac{\sqrt{\frac{7}{15}}}{4}&0&0&0&0&0&0&0&0&0\\0&-\frac{1}{12}&0&\frac{\sqrt{\frac{239}{35}}}{24}&0&0&0&0&0&0&0&0\\-\frac{\sqrt{\frac{5}{21}}}{8}&0&\frac{1}{16}&0&\frac{\sqrt{\frac{1943}{3}}}{672}&0&0&0&0&0&0&0\\0&\frac{5\sqrt{\frac{35}{239}}}{48}&0&\frac{1}{30}&0&\frac{\sqrt{\frac{1291}{15774}}}{10}&0&0&0&0&0&0\\-\frac{\sqrt{\frac{35}{1943}}}{8}&0&\frac{7\sqrt{\frac{3}{1943}}}{40}&0&\frac{1}{48}&0&0&0&0&0&0&0\\0&-\frac{\sqrt{\frac{385}{7746}}}{16}&0&\frac{\sqrt{\frac{2629}{7746}}}{160}&0&\frac{1}{70}&0&0&0&0&0&0\\0&0&0&0&0&0&-\frac{1}{8}&0&\frac{\sqrt{\frac{7}{15}}}{4}&0&0&0\\0&0&0&0&0&0&0&-\frac{1}{12}&0&\frac{\sqrt{\frac{239}{35}}}{24}&0&0\\0&0&0&0&0&0&-\frac{\sqrt{\frac{5}{21}}}{8}&0&\frac{1}{16}&0&\frac{\sqrt{\frac{1943}{3}}}{672}&0\\0&0&0&0&0&0&0&\frac{5\sqrt{\frac{35}{239}}}{48}&0&\frac{1}{30}&0&\frac{\sqrt{\frac{1291}{15774}}}{10}\\0&0&0&0&0&0&-\frac{\sqrt{\frac{35}{1943}}}{8}&0&\frac{7\sqrt{\frac{3}{1943}}}{40}&0&\frac{1}{48}&0\\0&0&0&0&0&0&0&-\frac{\sqrt{\frac{385}{7746}}}{16}&0&\frac{\sqrt{\frac{2629}{7746}}}{160}&0&\frac{1}{70}\end{bmatrix}$$

and

$$\overline{\vartheta'_{12}}(\xi) = \begin{bmatrix} 0 \\ 0 \\ 0 \\ 0 \\ \frac{\sqrt{\frac{1268209}{277849}}}{120}\vartheta_{1,6}(\xi) \\ \frac{\sqrt{\frac{2827883}{33566}}}{672}\vartheta_{1,7}(\xi) \\ 0 \\ 0 \\ 0 \\ 0 \\ \frac{\sqrt{\frac{1268209}{277849}}}{120}\vartheta_{2,6}(\xi) \\ \frac{\sqrt{\frac{2827883}{33566}}}{672}\vartheta_{2,7}(\xi) \end{bmatrix}.$$

The third integration can be written as:

$$\int_0^\xi \int_0^\xi \int_0^\xi \vartheta(\xi)\, d\xi = = \mathcal{B}''_{12\times 12}\ \vartheta_{12}(\xi) + \overline{\vartheta''_{12}(\xi)}, \tag{3.6}$$

where

$$\vartheta_{12}(\xi) = [\vartheta_{1,0}(\xi),\ \vartheta_{1,1}(\xi), \vartheta_{1,2}(\xi), \vartheta_{1,3}(\xi),\ \vartheta_{1,4}(\xi), \vartheta_{1,5}(\xi),\ \vartheta_{2,0}(\xi), \vartheta_{2,1}(\xi), \vartheta_{2,2}(\xi), \vartheta_{2,3}(\xi), \vartheta_{2,4}(\xi), \vartheta_{2,5}(\xi)]^T,$$

$$\mathcal{B}''_{12\times 12} = \begin{bmatrix}
0 & -\frac{1}{24\sqrt{3}} & 0 & \frac{\sqrt{\frac{239}{105}}}{48} & 0 & 0 & 0 & 0 & 0 & 0 & 0 & 0 \\
\frac{1}{32\sqrt{3}} & 0 & -\frac{\sqrt{\frac{7}{5}}}{32} & 0 & \frac{\sqrt{\frac{1943}{105}}}{192} & 0 & 0 & 0 & 0 & 0 & 0 & 0 \\
0 & -\frac{\sqrt{\frac{5}{7}}}{64} & 0 & \frac{\sqrt{239}}{1120} & 0 & \frac{\sqrt{\frac{1291}{66}}}{840} & 0 & 0 & 0 & 0 & 0 & 0 \\
\frac{\sqrt{\frac{105}{239}}}{64} & 0 & -\frac{49}{160\sqrt{239}} & 0 & \frac{\sqrt{\frac{1943}{717}}}{192} & 0 & 0 & 0 & 0 & 0 & 0 & 0 \\
0 & -\frac{3\sqrt{\frac{21}{9715}}}{32} & 0 & \frac{\sqrt{\frac{239}{5829}}}{80} & 0 & \frac{3\sqrt{\frac{1291}{42746}}}{140} & 0 & 0 & 0 & 0 & 0 & 0 \\
\frac{3\sqrt{\frac{385}{2582}}}{256} & 0 & -\frac{133\sqrt{\frac{11}{7746}}}{640} & 0 & \frac{\sqrt{\frac{21373}{2582}}}{1792} & 0 & 0 & 0 & 0 & 0 & 0 & 0 \\
0 & 0 & 0 & 0 & 0 & 0 & 0 & -\frac{1}{24\sqrt{3}} & 0 & \frac{\sqrt{\frac{239}{105}}}{48} & 0 & 0 \\
0 & 0 & 0 & 0 & 0 & 0 & \frac{1}{32\sqrt{3}} & 0 & -\frac{\sqrt{\frac{7}{5}}}{32} & 0 & \frac{\sqrt{\frac{1943}{105}}}{192} & 0 \\
0 & 0 & 0 & 0 & 0 & 0 & 0 & -\frac{\sqrt{\frac{5}{7}}}{64} & 0 & \frac{\sqrt{239}}{1120} & 0 & \frac{\sqrt{\frac{1291}{66}}}{840} \\
0 & 0 & 0 & 0 & 0 & 0 & \frac{\sqrt{\frac{105}{239}}}{64} & 0 & -\frac{49}{160\sqrt{239}} & 0 & \frac{\sqrt{\frac{1943}{717}}}{192} & 0 \\
0 & 0 & 0 & 0 & 0 & 0 & 0 & -\frac{3\sqrt{\frac{21}{9715}}}{32} & 0 & \frac{\sqrt{\frac{239}{5829}}}{80} & 0 & \frac{3\sqrt{\frac{1291}{42746}}}{140} \\
0 & 0 & 0 & 0 & 0 & 0 & \frac{3\sqrt{\frac{385}{2582}}}{256} & 0 & -\frac{133\sqrt{\frac{11}{7746}}}{640} & 0 & \frac{\sqrt{\frac{21373}{2582}}}{1792} & 0
\end{bmatrix}$$

and

$$\overline{\vartheta_{12}''}(\xi)=\begin{bmatrix}0\\0\\0\\0\\\frac{\sqrt{\frac{1268209}{277849}}}{120}\vartheta_{1,6}(\xi)\\\frac{\sqrt{\frac{2827883}{33566}}}{672}\vartheta_{1,7}(\xi)\\0\\0\\0\\0\\\frac{\sqrt{\frac{1268209}{277849}}}{120}\vartheta_{2,6}(\xi)\\\frac{\sqrt{\frac{2827883}{33566}}}{672}\vartheta_{2,7}(\xi)\end{bmatrix}.$$

We can similarly create matrices for our convenience.

4. Fibonacci wavelet method

Consider the generalized system of nonlinear ODE of the form:

$$y_r^{(p)}(\xi)=f\left(\xi,y_r,y_r^1,\ldots,y_r^{(p-1)}\right), \tag{4.1}$$

where (p) represents the order of the derivatives and $1\leq r\leq n$ and $1\leq p\leq k$. Concerning the primary constraints:

$$\left.\begin{aligned}y_r^{(p-1)}(0)&=b_{r,p-1,},\\y_r^{(p-2)}(0)&=b_{r,p-2,},\\&\vdots\\y_r(0)&=b_{r,0},\end{aligned}\right\} \tag{4.2}$$

where $b_{r,p-1},\ldots,\ b_{r,0}$ are constants. Assume that

$$y_r^{(p)}(\xi)=\sum_{i=0}^{\infty}\sum_{j=1}^{\infty}a_{i,j}^r\ \vartheta_{i,j}(\xi). \tag{4.3}$$

Truncating (4.3), we get,

$$y_r^{(p)}(\xi)\approx\sum_{i=0}^{k-1}\sum_{j=1}^{M-1}a_{i,j}^r\ \vartheta_{i,j}(\xi). \tag{4.4}$$

Integrating (4.4) concerning ξ once from 0 to ξ, we obtain,

$$y_r^{(p-1)}(\xi) \approx y_r^{(p-1)}(0) + A^T \left[\mathcal{B}\ \vartheta(\xi) + \overline{\vartheta(\xi)}\right].$$

From (4.2), we get,

$$\left.\begin{array}{l} y_r^{(p-1)}(\xi) \approx b_{r,p-1} + A^T \left[\mathcal{B}\ \vartheta(\xi) + \overline{\vartheta(\xi)}\right], \\ y_r^{(p-2)}(\xi) \approx b_{r,p-2} + \xi\ b_{r,p-1} + A^T \left[\mathcal{B}'\ \vartheta(\xi) + \overline{\vartheta'(\xi)}\right], \\ \quad \vdots \\ y'_r(\xi) \approx b_{r,1} + \xi\ b_{r,2} + \frac{\xi^2}{2!}\ b_{r,3} + , \ldots + \frac{\xi^{p-2}}{(p-2)!}\ b_{r,p-1} + A^T \left[\mathcal{B}^{(p-2)}\ \vartheta(\xi) + \overline{\vartheta^{(p-2)}(\xi)}\right], \\ y_r(\xi) \approx b_{r,0} + \xi\ b_{r,1} + \frac{\xi^2}{2!}\ b_{r,2} + \frac{\xi^3}{3!}\ b_{r,3} + , \ldots + \frac{\xi^{p-1}}{(p-1)!}\ b_{r,p-1} A^T \left[\mathcal{B}^{(p-1)}\ \vartheta(\xi) + \overline{\vartheta^{(p-1)}(\xi)}\right]. \end{array}\right\} \tag{4.5}$$

Now fit (4.4) and (4.5) in (4.1) and use the following grid points to collocate $x_i = \frac{2i-1}{2^k M}, i = 1, 2, \ldots, M$ and solve the collocated equations by the Newton-Raphson method, which provides the values of unknown Fibonacci wavelet coefficients. Substituting these coefficient values into y_r in (4.5) yields the Fibonacci wavelet numerical solution for system (4.1).

For fractional order: Fractionally differentiating y_r in (4.5) by using the Riemann-Liouville fractional derivative, we obtain

$$\begin{aligned} y_r^{\alpha_i}(\xi) \approx & \frac{d^{\alpha_i}}{d\xi^{\alpha_i}} (b_{r,0} + \xi\ b_{r,1} + \frac{\xi^2}{2}\ b_{r,2} + \frac{\xi^3}{3}\ b_{r,3} + , \ldots + \frac{\xi^{p-1}}{(p-1)!}\ b_{r,p-1} \\ & + A^T \left[\mathcal{B}^{(p-1)}\ \vartheta(\xi) + \overline{\vartheta^{(p-1)}(\xi)}\right]), \end{aligned} \tag{4.6}$$

where α_i is a non-integer order. Substitute (4.6) and y_r in (4.5) into (4.1) and collocate the obtained algebraic equations by equispaced grid points $\xi_i = \frac{2i-1}{2^k M}$, $i = 1, 2, \ldots, M$. By resolving the system mentioned above, we can determine the values of the unknown coefficients. Substituting these coefficient values into y_r of (4.5) produces the Fibonacci wavelet fractional numerical solution for the SFDEs (4.1).

Computational Algorithm

Step 1: Start.
Step 2:: Input the wavelet functions $\vartheta(\xi)$ and unknown coefficients A and B.
Step 3: Assume $Dy_1(\xi) = A^T\ \vartheta(\xi)$ and $Dy_2(\xi) = B^T\ \vartheta(\xi)$.
Step 4: Input the operational matrices $\mathcal{B}$ and $\overline{\vartheta(\xi)}$ extracted from the wavelet functions.
Step 5: Integrate the set of equations assumed in Step 3 concerning the independent variable ξ ranging from 0 to ξ.
Step 6: Replacing the integral terms of Step 5 with the operational matrices obtained in Step 3 and Step 4 and expressing the given initial conditions as wavelet functions, such as $y_1(0) = C^T\ \vartheta(\xi)$, and $y_2(0) = E^T\ \vartheta(\xi)$, we obtain

$$y_1(\xi) = C^T\ \vartheta(\xi) + A^T \left[\mathcal{B}\ \vartheta(\xi) + \overline{\vartheta(\xi)}\right]$$

and

$$y_2(\xi) = E^T\ \vartheta(\xi) + B^T \left[\mathcal{B}\ \vartheta(\xi) + \overline{\vartheta(\xi)}\right] + A^T \left[\mathcal{B}\ \vartheta(\xi) + \overline{\vartheta(\xi)}\right].$$

Step 7: Differentiating Step 6 fractionally concerning ξ using the Riemann-Liouville fractional derivative definition, we obtain

$$D_{\xi}^{\alpha_1}\left(y_1\left(\xi\right)\right) = D_{\xi}^{\alpha_1} C^T\ \vartheta\left(\xi\right) + A^T\left[\mathcal{B}\ \vartheta\left(\xi\right) + \ \overline{\vartheta\left(\xi\right)}\right]$$

and

$$D_{\xi}^{\alpha_1}\left(y_2\left(\xi\right)\right) = D_{\xi}^{\alpha_1} E^T\ \vartheta\left(\xi\right) + B^T\left[\mathcal{B}\ \vartheta\left(\xi\right) + \ \overline{\vartheta\left(\xi\right)}\right].$$

Step 8: Substitute Step 7, Step 6, and Step 3 into the considered system and collocate the system with the collocation points $\xi_i = \frac{2i-1}{2^k M},\ \ i = 1,\ 2, \ldots, M$.
Step 9: Apply the Newton-Raphson method to solve the algebraic equations derived from Step 8 for the unknown coefficients.
Step 10: Replace the unknown coefficients from Step 9 in Step 6 to obtain the wavelet solution of the considered system of FDEs.
Step 11: Stop.

5. Numerical illustration

We provide some examples to show the applicability and usefulness of this technique. The symbolic calculus programmer Mathematica is used to compute all the results.
Application 5.1: Let us consider a linear system of FDEs [8]:

$$\left.\begin{array}{l} D^{\alpha_1} y_1\left(\xi\right) = y_1\left(\xi\right) + y_2(\xi) \\ D^{\alpha_2} y_2\left(\xi\right) = -y_1\left(\xi\right) + y_2(\xi) \end{array}\right\}, \tag{5.1}$$

subject to the primary constraints $y_1\left(0\right) = 0,\ \ y_2\left(0\right) = 1$, where the parameters α_1 and α_2 are the fractional orders of time derivative with $0 \leq \alpha_1,\ \alpha_2 \leq 1$.The exact solutions are given by $y_1\left(\xi\right) = e^{\xi}\sin(\xi)$ and $y_2\left(\xi\right) = e^{\xi}\cos(\xi)$ for $\alpha_1 = \alpha_2 = 1$. The FWCM solutions for system (5.1) were produced for $\alpha_1 = \alpha_2 = 1$ and are displayed in Figures.1-3, which indicates that the solutions from the suggested method are reasonably similar to the actual outcomes. Numerical approximations obtained by FWCM are compared with the exact solution, and absolute errors of the developed approach with the exact solution are tabulated in Tables 1-4. As we increase the values of M and k, the FWCM solutions are calculated at various values, and the results get even more precise, as shown in Tables 1-4. The graphical depictions of the numerical simulations and the absolute error analysis are shown in Figures 3-6. It is evident from the tables and graphs that the FWCM method surpasses all other methods in getting the numerical approximations and produces a suitable result for the FDE linear system.

Table 1. Numerical outcomes attained using the FWCM and compared with exact solutions for $y_1(\xi)$ in Application 5.1.

ξ	**Exact Solution**	**FWCM Solution**			
		M=6, k=1	**M=6, k=2**	**M=10, k=1**	**M=10, k=2**
0	0.00000000000	0.00000000000	0.00000000000	0.00000000000	0.000000000000
0.1	0.11033298873	0.11033355921	0.11033299425	0.11033298872	0.110332988730
0.2	0.24265526859	0.24265539314	0.24265527385	0.24265526859	0.242655268594
0.3	0.39891055377	0.39891041150	0.39891055729	0.39891055377	0.398910553778
0.4	0.58094390077	0.58094349379	0.58094390335	0.58094390077	0.580943900770
0.5	0.79043908321	0.79043825998	0.79043908322	0.79043908322	0.790439083214
0.6	1.02884566627	1.02884436988	1.02884566449	1.02884566628	1.028845666270
0.7	1.29729511188	1.29729335144	1.29729510752	1.29729511189	1.297295111880
0.8	1.59650534060	1.59650295782	1.59650533298	1.59650534062	1.596505340600
0.9	1.92667330397	1.92667005326	1.92667329259	1.92667330400	1.926673303970
1.0	2.28735528718	2.28735202773	2.28735527231	2.28735528721	2.287355287180

Table 2. Numerical outcomes attained using the FWCM and compared with exact solutions for $y_2(\xi)$ in Application 5.1.

ξ	**Exact Solution**	**FWCM Solution**			
		M=6, k=1	**M=6, k=2**	**M=10, k=1**	**M=10, k=2**
0	0.00000000000	0.00000000000	0.00000000000	0.00000000000	0.00000000000
0.1	1.09964966683	1.09964672225	1.09964965444	1.09964966685	1.09964966682
0.2	1.19705602136	1.19705352847	1.19705600621	1.19705602138	1.19705602135
0.3	1.28956937404	1.28956666921	1.28956935794	1.28956937407	1.28956937404
0.4	1.37406153889	1.37405835592	1.37406151972	1.37406153892	1.37406153888
0.5	1.44688903658	1.44688568066	1.44688903661	1.44688903661	1.44688903658
0.6	1.50385954056	1.50385604611	1.50385951830	1.50385954059	1.50385954056
0.7	1.54020302543	1.54019910587	1.54020299940	1.54020302547	1.54020302543
0.8	1.55054929681	1.55054521498	1.55054927076	1.55054929684	1.55054929681
0.9	1.52891381188	1.52891039076	1.52891378214	1.52891381192	1.52891381188
1.0	1.46869393992	1.46868778396	1.46869388879	1.46869393997	1.46869393992

Table 3. The A.E. of FWCM solution of $y_1(\xi)$ for Application 5.1

ξ	**Exact Solution**	**Absolute Error**			
		M=6, k=1	**M=6, k=2**	**M=10, k=1**	**M=10, k=2**
0	0.00000000000	0	0	0	0
0.1	0.11033298873	5.70×10^{-7}	5.52×10^{-9}	3.82×10^{-12}	3.24×10^{-15}
0.2	0.24265526859	1.24×10^{-7}	5.25×10^{-9}	1.68×10^{-12}	2.80×10^{-15}
0.3	0.39891055377	1.42×10^{-7}	3.51×10^{-9}	6.08×10^{-13}	2.22×10^{-15}
0.4	0.58094390077	4.06×10^{-7}	2.58×10^{-9}	3.44×10^{-12}	1.55×10^{-15}
0.5	0.79043908321	8.23×10^{-7}	6.82×10^{-9}	6.82×10^{-12}	2.33×10^{-15}
0.6	1.02884566627	1.29×10^{-7}	1.78×10^{-9}	1.07×10^{-11}	8.88×10^{-16}
0.7	1.29729511188	1.76×10^{-6}	4.35×10^{-9}	1.54×10^{-11}	8.88×10^{-16}
0.8	1.59650534060	2.38×10^{-6}	7.61×10^{-9}	2.06×10^{-11}	3.10×10^{-15}
0.9	1.92667330397	3.25×10^{-6}	1.13×10^{-9}	2.70×10^{-11}	6.21×10^{-15}
1.0	2.28735528718	3.25×10^{-6}	1.48×10^{-9}	2.83×10^{-11}	9.76×10^{-15}

Table 4. The A.E. of FWCM solution of $y_2(\xi)$ for Application 5.1

ξ	**Exact Solution**	**Absolute Error**			
		M=6, k=1	**M=6, k=2**	**M=10, k=1**	**M=10, k=2**
0	0.00000000000	0	0	0	0
0.1	1.09964966683	2.94×10^{-6}	1.23×10^{-8}	2.11×10^{-11}	6.66×10^{-15}
0.2	1.19705602136	2.49×10^{-6}	1.51×10^{-8}	2.25×10^{-11}	7.77×10^{-15}
0.3	1.28956937404	2.70×10^{-6}	1.61×10^{-8}	2.51×10^{-11}	8.88×10^{-15}
0.4	1.37406153889	3.18×10^{-6}	1.91×10^{-8}	2.75×10^{-11}	1.04×10^{-14}
0.5	1.44688903658	3.35×10^{-6}	2.98×10^{-8}	2.98×10^{-11}	5.55×10^{-15}
0.6	1.50385954056	3.49×10^{-6}	2.22×10^{-8}	3.21×10^{-11}	1.93×10^{-14}
0.7	1.54020302543	3.91×10^{-6}	2.60×10^{-8}	3.40×10^{-11}	2.15×10^{-14}
0.8	1.55054929681	4.08×10^{-6}	2.60×10^{-8}	3.59×10^{-11}	2.35×10^{-14}
0.9	1.52891381188	3.42×10^{-6}	2.97×10^{-8}	3.62×10^{-11}	2.57×10^{-14}
1.0	1.46869393992	6.15×10^{-6}	5.11×10^{-8}	5.56×10^{-11}	3.93×10^{-14}

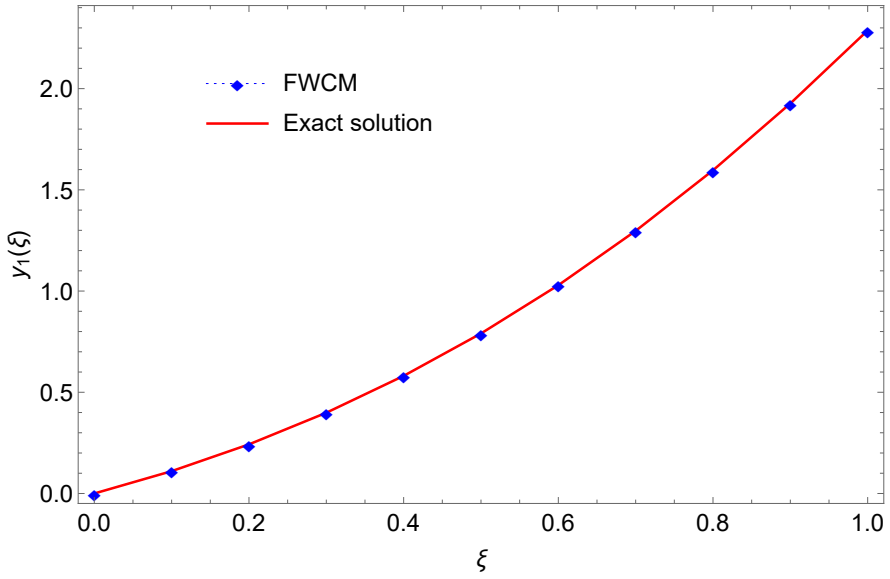

Figure 1. Plot of the solution $y_1(\xi)$ of Application 5.1.

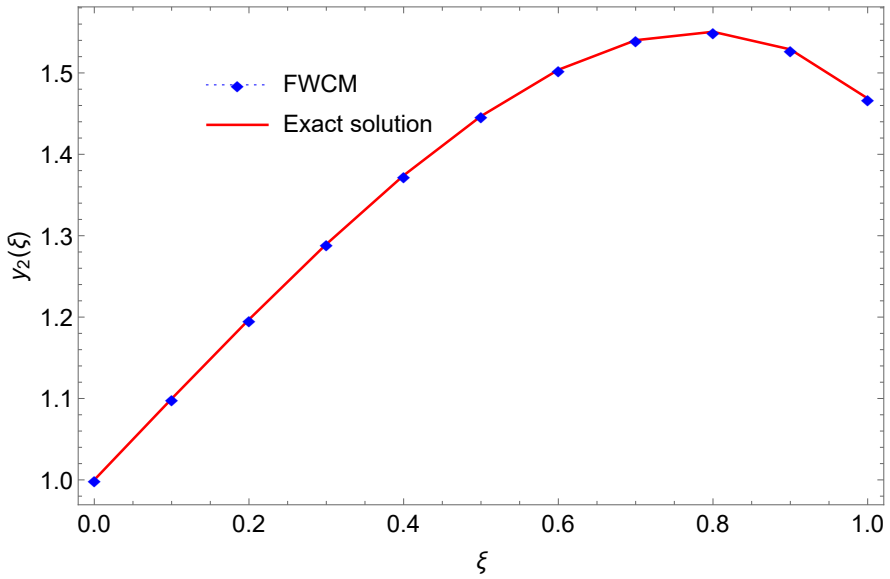

Figure 2. Plot of the solution $y_2(\xi)$ of Application 5.1.

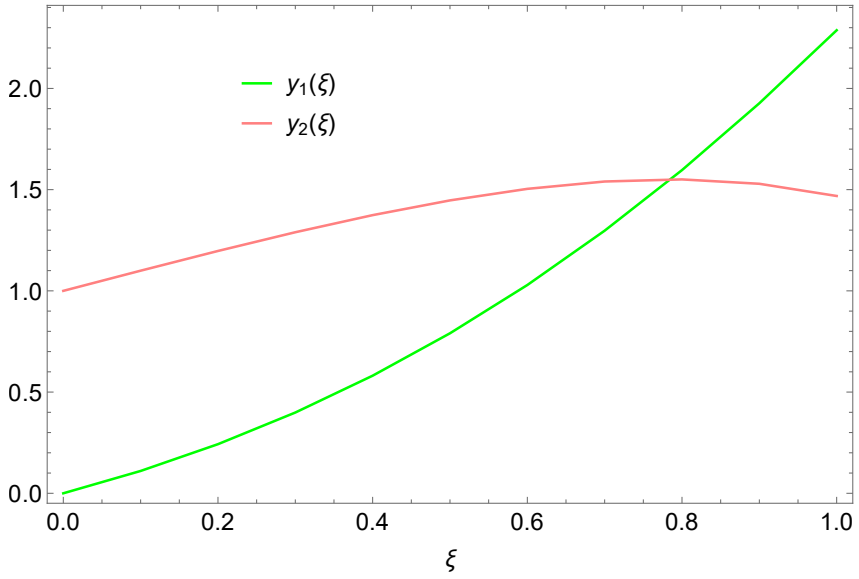

Figure 3. Plots of the system (5.1) when $\alpha_1 = \alpha_2 = 1$ by the present method.

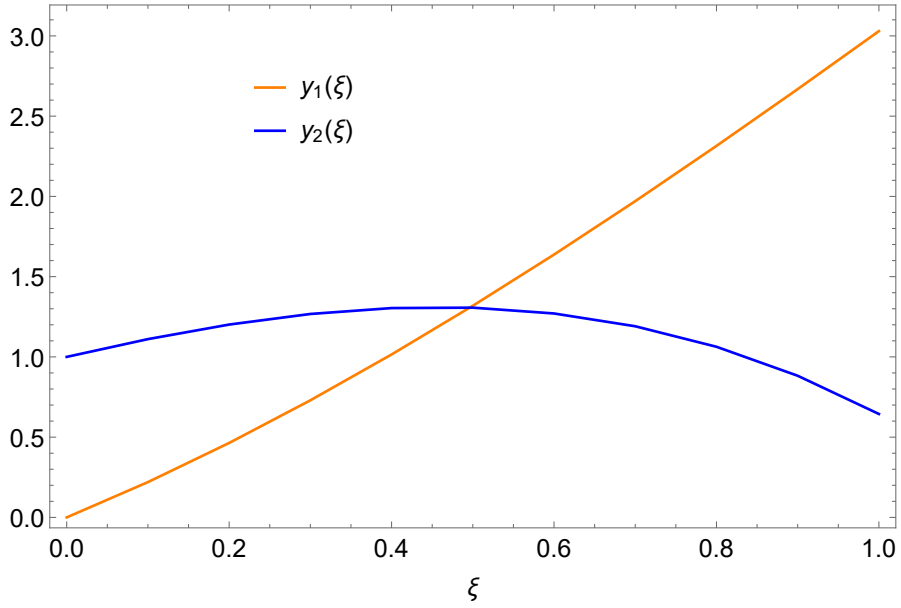

Figure 4. Plots of the system (5.1) when $\alpha_1 = 0.7, \alpha_2 = 0.9$ by the FWCM.

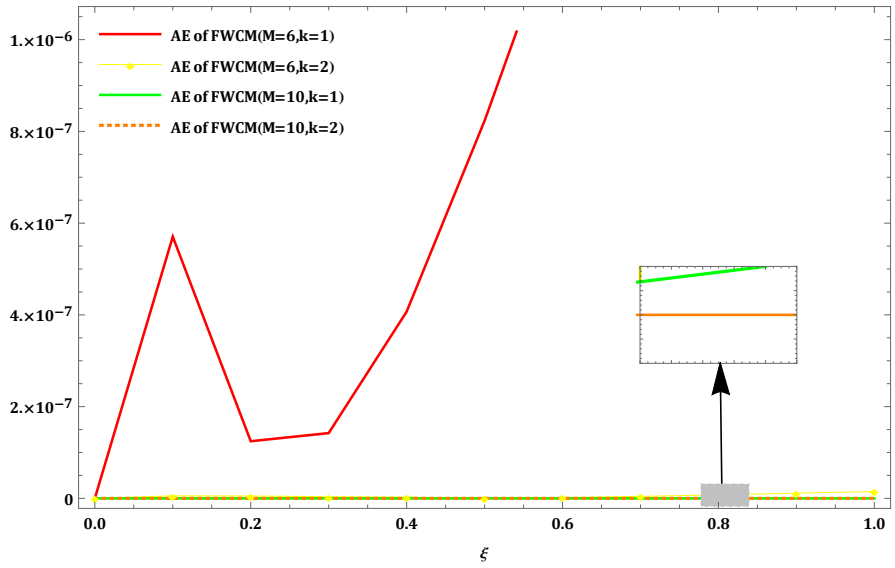

Figure 5. Comparsion of AE for $y_1(\xi)$ at diverse values of M and k for Application (5.1).

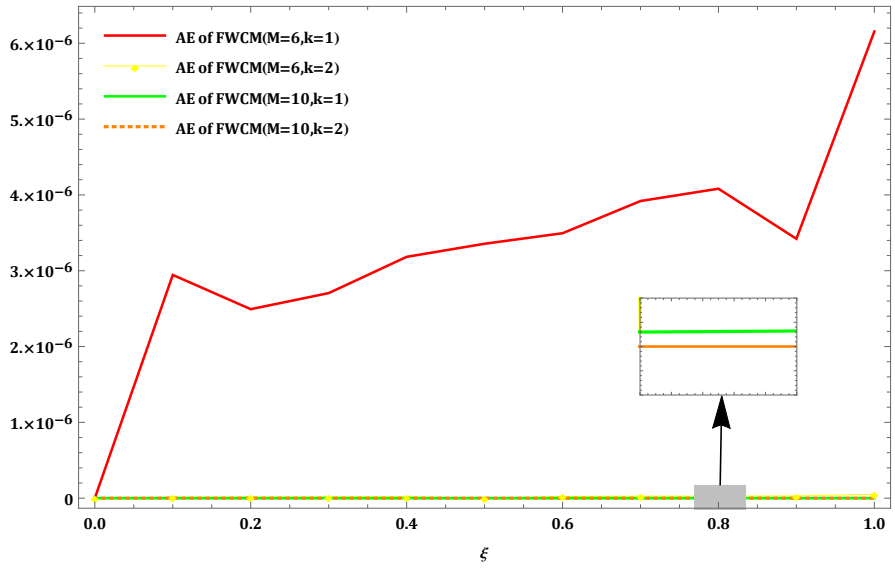

Figure 6. PComparsion of AE for $y_2(\xi)$ at diverse values of M and k for Application (5.1).

Application 5.2: Next, we consider the system of two nonlinear FDEs [8]:

$$\left.\begin{aligned} D^{\alpha_1} y_1(\xi) &= y_1(\xi) + y_2(\xi)^2 \\ D^{\alpha_2} y_1(\xi) &= y_1(\xi) + 5\, y_2(\xi) \end{aligned}\right\}, \tag{5.2}$$

subject to the primary constraints: $y_1(0) = 0, \quad y_2(0) = 0, \quad y'_1(0) = 0, \quad y'_2(0) = 1, \quad y''_2(0) = 1$. The numerical approximations of integer order obtained for the system (5.2) are shown in Tables 5-6. Graphical representations of the attained solution from the developed approach are drawn in Figures 7-9. The A.E. of the developed technique with the NDSolver with distinct values of M and k are shown in Figure 9. In the graph, the flat line indicates that on increasing the values of M and k, we will attain a better-approximated solution than the solution obtained from the previous values of M and k. Also, methods such as ADM [2], the DTM [3], and the HPM [6] all produce findings that are incredibly close to the graphic results shown in Figures 7-8.

Table 5. : Numerical solution and Absolute errors of $y_1(\xi)$ for integer order ($\alpha_1 = 2, \quad \alpha_2 = 3$).

ξ	**N.D.Solve**	**FWCM (M=6)**		**FWCM (M=10)**	
	Solution	**Solution**	**AE**	**Solution**	**AE**
0	0.00000000000	0.00000000000	0	0.000000000000	0
0.1	0.10017559486	0.10016460090	1.09×10^{-5}	0.100175591299	3.56×10^{-9}
0.2	0.20148623331	0.20146312296	2.31×10^{-5}	0.201486221959	1.13×10^{-8}
0.3	0.30532818974	0.30529526528	3.29×10^{-5}	0.305328169131	2.06×10^{-8}
0.4	0.41346899510	0.41342491367	4.40×10^{-5}	0.413468956244	3.88×10^{-8}
0.5	0.52816870803	0.52811264824	5.60×10^{-5}	0.528168661027	4.70×10^{-8}
0.6	0.65234460498	0.65227689599	6.77×10^{-5}	0.652344539923	6.50×10^{-8}
0.7	0.78980008071	0.78971951723	8.05×10^{-5}	0.789799992022	8.86×10^{-8}
0.8	0.94554716550	0.94545161425	9.55×10^{-5}	0.945547044962	1.20×10^{-7}
0.9	1.12626348963	1.12615535092	1.08×10^{-4}	1.126263325160	1.64×10^{-7}
1.0	1.34094172277	1.34081757177	1.24×10^{-4}	1.340941513800	2.08×10^{-7}

Table 6. : Numerical solution and Absolute errors of $y_2(\xi)$ for integer order ($\alpha_1 = 2, \quad \alpha_2 = 3$).

ξ	**N.D.Solve**	**FWCM (M=6)**		**FWCM (M=10)**	
	Solution	**Solution**	**AE**	**Solution**	**AE**
0	0.00000000000	0.00000000000	0	0.000000000000	0
0.1	0.10502542748	0.10502533963	8.78×10^{-8}	0.105025418679	8.80×10^{-9}
0.2	0.22041351408	0.22041311166	4.02×10^{-7}	0.220413505463	8.61×10^{-9}
0.3	0.34712871329	0.34712778748	9.25×10^{-7}	0.347128704034	9.25×10^{-9}
0.4	0.48684330725	0.48684162506	1.68×10^{-6}	0.486843294238	1.30×10^{-8}
0.5	0.64200163771	0.64199890974	2.72×10^{-6}	0.642001623782	1.39×10^{-8}
0.6	0.81589666320	0.81589254122	4.12×10^{-6}	0.815896645461	1.77×10^{-8}
0.7	1.01276340925	1.01275747552	5.93×10^{-6}	1.012763386500	2.27×10^{-8}
0.8	1.23789462779	1.23788634490	8.28×10^{-6}	1.237894598455	2.93×10^{-8}
0.9	1.49778467249	1.49777339279	1.12×10^{-5}	1.497784634547	3.79×10^{-8}
1.0	1.80030868801	1.80029367483	1.50×10^{-5}	1.800308640164	4.78×10^{-8}

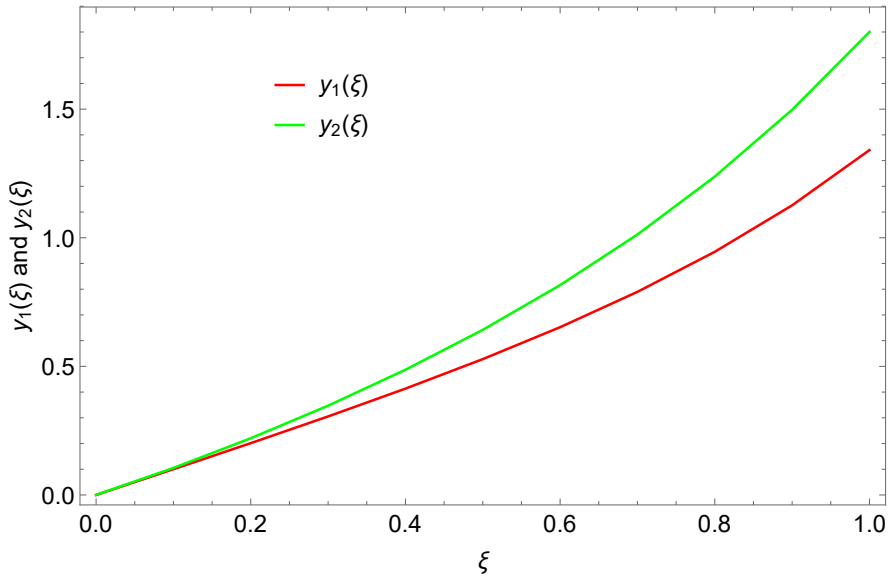

Figure 7. Plots of the system (5.2) by the present method for the integer order ($\alpha_1 = 2, \alpha_2 = 3$).

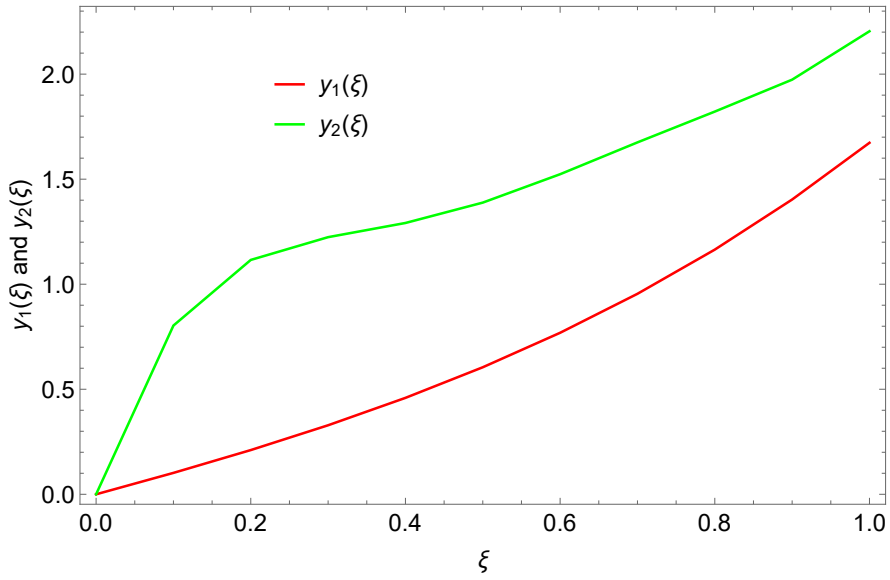

Figure 8. Plots of the system (5.2) by the present method for the fractional order $(\alpha_1 = 1.3, \alpha_2 = 2.4)$**.**

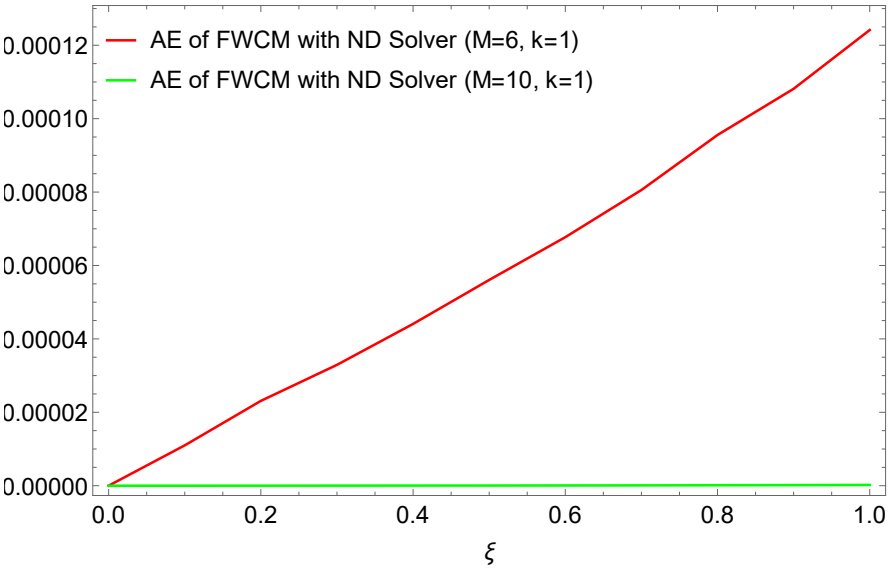

Figure 9. Plot of A.E. for Application (5.2) for integer order $(\alpha_1 = 2, \alpha_2 = 3)$**.**

Application 5.3: Consider the following nonlinear system of three nonlinear FDEs [8]:

$$\left.\begin{array}{l} D^{\alpha_1} y_1(\xi) = 2\, y_2(\xi)^2 \\ D^{\alpha_2} y_2(\xi) = \xi\, y_1(\xi) \\ D^{\alpha_3} y_3(\xi) = y_1(\xi)\; y_3(\xi) \end{array}\right\}, \tag{5.3}$$

concerning primary constraints: $y_1(0) = 0, \quad y_2(0) = 1, \quad y_3(0) = 1.$

Since the exact solution is unavailable, numerical approximations produced by the suggested scheme (FWCM) are compared with the NDSolve solution; the absolute errors of the method used with NDSolve are listed in Tables 7-13. The results produced from the ADM method [2], DTM method [3], and HPM method [6] agree well with the graphical results shown in Figures 10-11. The graphical depictions of A.E. analysis combined with numerical simulations are shown in Figures 12-14. Tables and graphs show that the FWCM approach provides a reasonable solution for the system of FDEs and is appropriate for producing the numerical approximation.

Table 7. Numerical approximation of $y_1(\xi)$ when $\alpha_1 = \alpha_2 = \alpha_3 = 1$.

ξ	**N.D. Solve**	**FWCM Solution**			
	Solution	**M=6, k=1**	**M=6, k=2**	**M=10, k=1**	**M=10, k=2**
0	0.00000000000	0.00000000000	0.00000000000	0.00000000000	0.00000000000
0.1	0.20006669136	0.19930020585	0.20098865323	0.20006240454	0.20006668552
0.2	0.40106911772	0.40044846436	0.40154650043	0.40106471688	0.40106910844
0.3	0.60544190861	0.60477361859	0.60593757897	0.60543707804	0.60544188300
0.4	0.81738272311	0.81657493749	0.81842592621	0.81737754691	0.81738278613
0.5	1.04319276127	1.04232571424	1.04232571424	1.04318707526	1.04319276127
0.6	1.29197221296	1.29102949299	1.29738183918	1.29196575351	1.29197210671
0.7	1.57690317942	1.57572892381	1.57976496076	1.57689615527	1.57690341373
0.8	1.91753779918	1.91616724603	1.92096745101	1.91752887685	1.91753746044
0.9	2.34388200058	2.34260239989	2.35248168201	2.34387178833	2.34388179201
1.0	2.90393454742	2.90077376644	2.90580002580	2.90391248542	2.90393370193

Table 8. Numerical approximation of $y_2(\xi)$ when $\alpha_1 = \alpha_2 = \alpha_3 = 1$.

ξ	**N.D. Solve**	**FWCM Solution**			
	Solution	**M=6, k=1**	**M=6, k=2**	**M=10, k=1**	**M=10, k=2**
0	1.00000000000	1.00000000000	1.00000000000	1.00000000000	1.00000000000
0.1	1.00066676947	1.00047333751	1.00076370473	1.00066592041	1.00066677774
0.2	1.00534045117	1.00519665526	1.00538558961	1.00533958271	1.00534045524
0.3	1.01808142141	1.01792492659	1.01813853592	1.01808042213	1.01808141820
0.4	1.04312736090	1.04292573368	1.04329542494	1.04312620987	1.04312737951
0.5	1.08511153347	1.08488149268	1.08488149268	1.08511015178	1.08511153348
0.6	1.14940441084	1.14913497954	1.15128926063	1.14940267223	1.14940438028
0.7	1.24263902594	1.24227815645	1.24370564645	1.24263695833	1.24263910663
0.8	1.37353749344	1.37308429892	1.37481246893	1.37353463216	1.37353738002
0.9	1.55425553193	1.55378342349	1.55729154688	1.55425196790	1.55425544853
1.0	1.80267769894	1.80168101611	1.80382469911	1.80267137259	1.80267741216

Table 9. Numerical approximation of $y_3(\xi)$ when $\alpha_1 = \alpha_2 = \alpha_3 = 1$.

ξ	**N.D. Solve**	**FWCM Solution**			
	Solution	**M=6, k=1**	**M=6, k=2**	**M=10, k=1**	**M=10, k=2**
0	1.00000000000	1.00000000000	1.00000000000	1.00000000000	1.00000000000
0.1	1.10518934701	1.10434845749	1.10518844815	1.10518246818	1.10518933922
0.2	1.22172877169	1.22102266025	1.22172767206	1.22172144863	1.22172875716
0.3	1.35168708404	1.35090070773	1.35168592333	1.35167878152	1.35168705644
0.4	1.49824266567	1.49726768625	1.49824132438	1.49823339540	1.49824271246
0.5	1.66619522901	1.66511237710	1.66618473230	1.66618473232	1.66619522901
0.6	1.86275664526	1.86154141262	1.86271286302	1.86274453725	1.86275651619
0.7	2.09884241646	2.09731088003	2.09878852397	2.09882871169	2.09884259330
0.8	2.39129994706	2.38947537330	2.39123853678	2.39128306513	2.39129954895
0.9	2.76695697210	2.76515449278	2.76687793073	2.76693739114	2.76695666723
1.0	3.27047316491	3.26641679283	3.27032830789	3.27043398349	3.27047209735

Table 10. Absolute error of $y_1(\xi)$ with NDSolver solution for Application 5.3.

ξ	**N.D. Solve Solution**	**Absolute Error at**			
		M=6, k=1	**M=6, k=2**	**M=10, k=1**	**M=10, k=2**
0	0.00000000000	0	0	0	0
0.1	0.20006669136	7.66×10^{-4}	1.47×10^{-6}	4.28×10^{-6}	5.84×10^{-9}
0.2	0.40106911772	6.20×10^{-4}	1.32×10^{-6}	4.40×10^{-6}	9.27×10^{-9}
0.3	0.60544190861	6.68×10^{-4}	1.31×10^{-6}	4.83×10^{-6}	2.56×10^{-8}
0.4	0.81738272311	8.07×10^{-4}	1.43×10^{-6}	5.17×10^{-6}	6.30×10^{-8}
0.5	1.04319276127	8.67×10^{-4}	5.68×10^{-6}	5.68×10^{-6}	1.33×10^{-8}
0.6	1.29197221296	9.42×10^{-4}	3.09×10^{-5}	6.45×10^{-6}	1.06×10^{-9}
0.7	1.57690317942	1.17×10^{-4}	3.74×10^{-5}	7.02×10^{-6}	2.34×10^{-7}
0.8	1.91753779918	1.37×10^{-4}	4.19×10^{-5}	8.92×10^{-6}	3.38×10^{-7}
0.9	2.34388200058	1.27×10^{-4}	5.38×10^{-5}	1.02×10^{-5}	2.08×10^{-7}
1.0	2.90393454742	3.16×10^{-4}	1.07×10^{-4}	2.20×10^{-5}	8.45×10^{-7}

Table 11. Absolute error of $y_2(\xi)$ with NDSolver solution for Application 5.3.

ξ	**N.D. Solve Solution**	**Absolute Error at**			
		M=6, k=1	**M=6, k=2**	**M=10, k=1**	**M=10, k=2**
0	1.00000000000	0	0	0	0
0.1	1.00066676947	1.93×10^{-4}	1.64×10^{-7}	8.49×10^{-7}	8.27×10^{-9}
0.2	1.00534045117	1.43×10^{-4}	2.05×10^{-7}	8.68×10^{-7}	4.05×10^{-9}
0.3	1.01808142141	1.56×10^{-4}	2.22×10^{-7}	9.99×10^{-7}	3.21×10^{-9}
0.4	1.04312736090	2.01×10^{-4}	2.72×10^{-7}	1.15×10^{-6}	1.86×10^{-8}
0.5	1.08511153347	2.30×10^{-4}	1.38×10^{-6}	1.38×10^{-6}	1.55×10^{-8}
0.6	1.14940441084	2.69×10^{-4}	8.80×10^{-6}	1.73×10^{-6}	3.05×10^{-8}
0.7	1.24263902594	3.60×10^{-4}	1.14×10^{-5}	2.06×10^{-6}	8.06×10^{-8}
0.8	1.37353749344	4.53×10^{-4}	1.39×10^{-5}	2.86×10^{-6}	1.13×10^{-7}
0.9	1.55425553193	4.72×10^{-4}	1.86×10^{-5}	3.56×10^{-6}	8.34×10^{-8}
1.0	1.80267769894	9.96×10^{-4}	3.18×10^{-5}	6.32×10^{-6}	2.86×10^{-7}

Table 12. Absolute error of $y_3(\xi)$ with NDSolver solution for Application 5.3.

ξ	**N.D. Solve Solution**	**Absolute Error at**			
		M=6, k=1	**M=6, k=2**	**M=10, k=1**	**M=10, k=2**
0	1.00000000000	0	0	0	0
0.1	1.10518934701	8.40×10^{-4}	8.98×10^{-7}	6.87×10^{-6}	7.79×10^{-9}
0.2	1.22172877169	7.06×10^{-4}	1.09×10^{-6}	7.32×10^{-6}	1.45×10^{-8}
0.3	1.35168708404	7.86×10^{-4}	1.16×10^{-6}	8.30×10^{-6}	2.76×10^{-8}
0.4	1.49824266567	9.74×10^{-4}	1.34×10^{-6}	9.27×10^{-6}	4.67×10^{-8}
0.5	1.66619522901	1.08×10^{-3}	1.04×10^{-5}	1.04×10^{-5}	2.66×10^{-8}
0.6	1.86275664526	1.21×10^{-4}	4.37×10^{-5}	1.21×10^{-5}	1.29×10^{-7}
0.7	2.09884241646	1.53×10^{-3}	5.38×10^{-5}	1.37×10^{-5}	1.76×10^{-7}
0.8	2.39129994706	1.82×10^{-3}	6.14×10^{-5}	1.68×10^{-5}	3.98×10^{-7}
0.9	2.76695697210	$180. \times 10^{-3}$	7.90×10^{-5}	1.95×10^{-5}	3.04×10^{-7}
1.0	3.27047316491	4.05×10^{-3}	1.44×10^{-4}	3.91×10^{-5}	1.06×10^{-6}

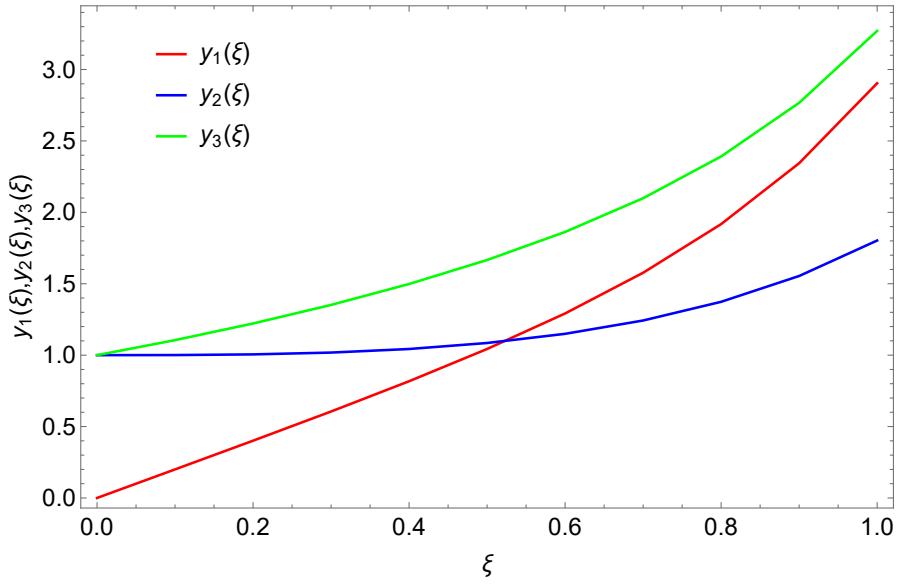

Figure 10. Plots of the system (5.3) by the present method when $\alpha_1 = \alpha_2 = \alpha_3 = 1$.

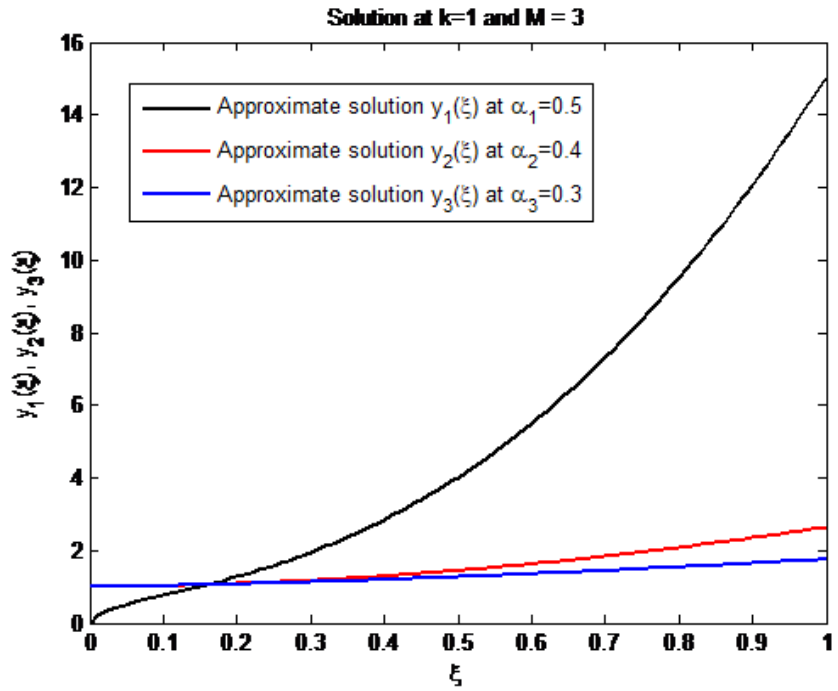

Figure 11. Plots of the system (5.3) by the FWCM when $\alpha_1 = 0.5, \quad \alpha_2 = 0.4, \quad \alpha_3 = 0.3.$

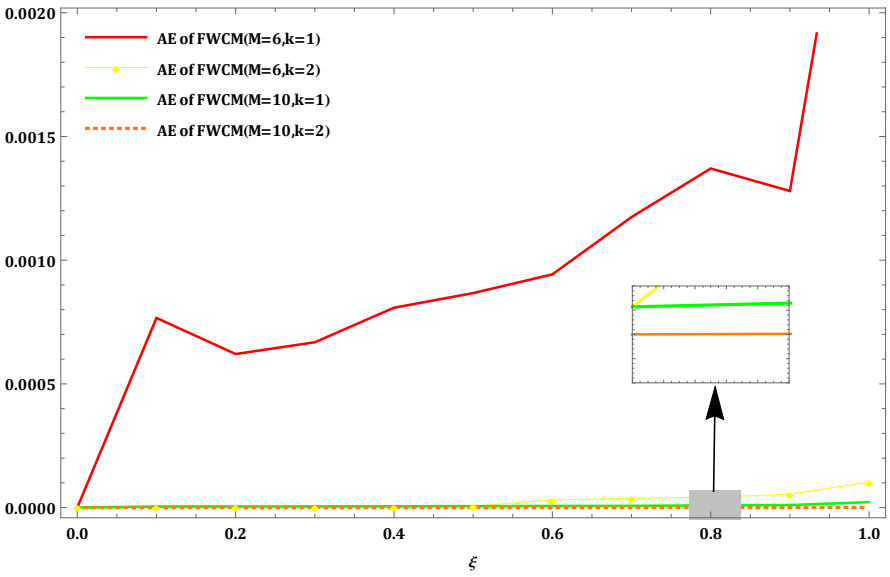

Figure 12. Comparision of the A.E. of the solution $y_1(\xi)$ **for Application (5.3).**

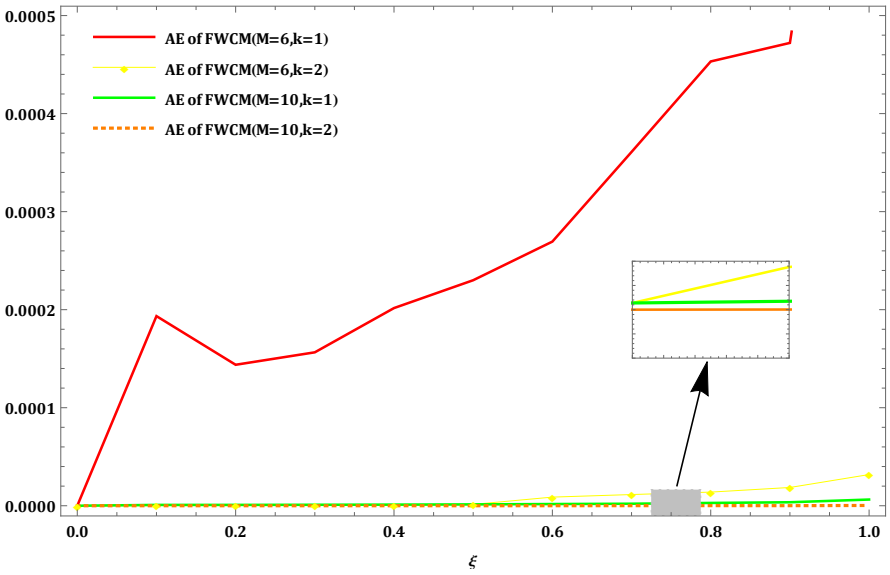

Figure 13. Comparision of the A.E. of the solution $y_2(\xi)$ for Application (5.3).

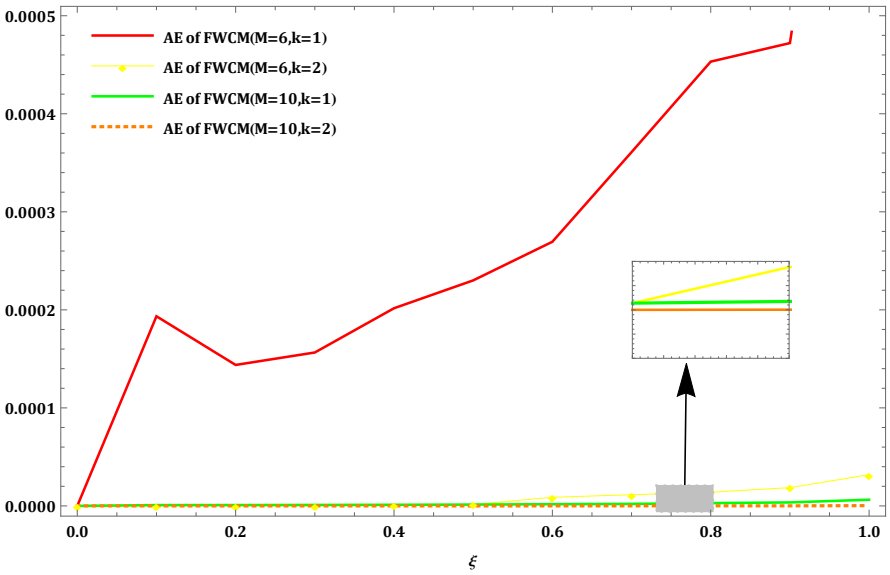

Figure 14. Comparision of the A.E. of the solution $y_3(\xi)$ for Application (5.3).

Application 5.4: Consider the following nonlinear system of two nonlinear FDEs:

[5]

$$\left.\begin{aligned} D^{\alpha_1} Y_1(\xi) &= -1002\, Y_1(\xi) + 1000\, Y_2^2(\xi) \\ D^{\alpha_2} Y_2(\xi) &= Y_1(\xi) - Y_2(\xi)(1 + Y_2(\xi)) \end{aligned}\right\}, \tag{5.4}$$

subject to the initial condition: $Y_1(0) = 1, \quad Y_2(0) = 1$. The exact solutions to the system when $\alpha_1 = \alpha_2 = 1$ are $Y_1(\xi) = e^{-2\xi}$ and $Y_2(\xi) = e^{\xi}$. The Fibonacci wavelet collocation method (FWCM) solutions shown in Tables 13-14 reveal that the proposed method solutions are reasonably close to the exact solution compared to the existing methods such as Chebyshev polynomials (CMCP), multistep fractional differential transform method (MSFDTM), fractional differential transform method (MSFDTM), Haar wavelet method and NDSolver. From the tables, it is clear that the FWCM method dominates all the other techniques in obtaining the numerical approximation and yields a satisfactory result for the desired system.

Table 13. Comparision of the A.E.of the solution $Y_1(\xi)$ for the application (5.4).

ξ	**AE of FWCM (M=10)**	**AE of MSFDTM** [5]	**AE of FDTM** [5]	**AE of Haar Wavelet Method**	**AE of CWCP (N=8)** [46]	**AE of N.D.Solver**
0	0	0	0	0	0	0
0.1	1.11×10^{-16}	-	-	8.10×10^{-6}	-	4.19×10^{-9}
0.2	3.33×10^{-16}	-	-	2.91×10^{-6}	0.45×10^{-8}	2.06×10^{-9}
0.3	1.11×10^{-16}	-	-	2.21×10^{-6}	-	6.18×10^{-9}
0.4	5.55×10^{-17}	-	-	1.67×10^{-6}	0.61×10^{-8}	8.78×10^{-9}
0.5	1.66×10^{-16}	1.66×10^{-15}	1.21×10^{-3}	1.25×10^{-6}	-	1.02×10^{-8}
0.6	1.11×10^{-16}	-	-	9.37×10^{-7}	0.10×10^{-8}	1.08×10^{-8}
0.7	2.77×10^{-17}	-	-	6.87×10^{-7}	-	1.09×10^{-8}
0.8	4.71×10^{-16}	-	-	4.99×10^{-7}	0.13×10^{-8}	1.06×10^{-8}
0.9	3.41×10^{-16}	-	-	2.50×10^{-7}	-	1.00×10^{-8}
1.0	3.26×10^{-16}	6.23×10^{-16}	6.86×10^{-2}	1.70×10^{-7}	0.53×10^{-7}	9.39×10^{-9}

Table 14. Comparision of the A.E.of the solution $Y_2(\xi)$ for the application (5.4).

ξ	**AE of FWCM (M=10)**	**AE of MSFDTM** [5]	**AE of FDTM** [5]	**AE of Haar Wavelet Method**	**AE of CWCP (N=8)** [46]	**AE of N.D.Solver**
0	0	0	0	0	0	0
0.1	1.10×10^{-16}	-	-	5.32×10^{-7}	-	2.18×10^{-9}
0.2	2.22×10^{-16}	-	-	6.32×10^{-7}	0.14×10^{-10}	1.38×10^{-9}
0.3	2.22×10^{-16}	-	-	4.32×10^{-6}	-	4.30×10^{-9}
0.4	1.11×10^{-16}	-	-	3.21×10^{-6}	0.21×10^{-10}	6.65×10^{-9}
0.5	2.22×10^{-16}	9.64×10^{-16}	2.02×10^{-5}	2.32×10^{-6}	-	8.51×10^{-9}
0.6	2.22×10^{-16}	-	-	1.65×10^{-7}	0.22×10^{-10}	9.97×10^{-9}
0.7	3.33×10^{-16}	-	-	1.87×10^{-7}	-	1.10×10^{-8}
0.8	3.88×10^{-16}	-	-	2.85×10^{-7}	0.18×10^{-10}	1.18×10^{-8}
0.9	3.88×10^{-16}	-	-	2.63×10^{-7}	-	1.24×10^{-8}
1.0	1.66×10^{-16}	8.54×10^{-16}	1.21×10^{-3}	3.62×10^{-7}	0.20×10^{-10}	1.28×10^{-8}

6. Conclusion

In this article, we have successfully implemented the Fibonacci wavelet collocation method for solving the system of fractional differential equations. Based on the Fibonacci wavelets, a new operational matrix is created for different resolutions (k) and combined with the collocation technique to solve the SFDEs numerically. FWCM solutions are computed for a range of M and k values. Tables 3-6 and 10-14 show that raising the values of M and k can yield greater accuracy in the results. The FWCM solutions for systems (5.1), (5.2), and (5.3) that were discovered for different values of α are shown in Figures $1, 2, 3, 4, 7, 8, 10$, and 11. The results of the developed strategy have been compared to those of the NDSolve and the exact solution. Four numerical examples are finally provided to show the suggested approach's accuracy. Examples demonstrate that when the exact solutions are known, the numerical solutions agree with the exact solutions. Also, numerical illustrations support the claim that only a few numerals of Fibonacci wavelets are sufficient to attain suitable outcomes. The present research underlined our conviction that the method is an appropriate method for handling fractional differential equations that are both linear and nonlinear.

Declarations

Availability of Data and Materials: The data supporting this study's findings are available within the article.
Competing interests: The authors declare that they have no competing interests.
Author's contributions: KS proposed the main idea of this paper. KS and MG prepared the manuscript and performed all the steps of the proofs in this research. Both authors contributed equally and significantly to writing this paper. Both authors read and approved the final manuscript.
Conflict of interest: The author declares no conflict of interest.
Funding: The author states that no funding is involved.

Acknowledgements

The author expresses his affectionate thanks to the DST-SERB, Govt. of India. New Delhi for the financial support under Empowerment and Equity Opportunities for Excellence in Science for 2023-2026. F.No.EEQ/2022/620 Dated:07/02/2023.

References

[1] S. Kumbinarasaiah, and M. Mulimani, *A novel scheme for the hyperbolic partial differential equation through Fibonacci wavelets*, Journal of Taibah University for Science, 2022, 16(1), 1112–1132.

[2] S. Momani and Z. Odibat, *Analytical approach to linear fractional partial differential equations arising in fluid mechanics*, Physics Letters A, 2006, 355(4-5), 271–279.

[3] H. Xu, *A generalized analytical approach for highly accurate solutions of fractional differential equations*, Chaos, Solitons and Fractals, 2023, 166, 112917.

[4] Z. Odibat and S. Kumar, *A robust computational algorithm using the homotopy asymptotic method for solving systems of fractional differential equations*, Journal of Computational and Nonlinear Dynamics, 2019, 14(8), 081004.

[5] H. A. Alkresheh and A. I. Ismail, *Multistep fractional differential transform method for the solution of fractional order stiff systems*, Ain Shams Engineering Journal, 2021, 12(4), 4223–4231.

[6] O. Abdulaziz, I. Hashim and S. Momani, *Solving systems of fractional differential equations by homotopy-perturbation method*, Physics Letters A, 2008, 372(4), 451–459.

[7] H. Jafari and V. Daftardar-Gejji, *Solving a system of nonlinear fractional differential equations using Adomian decomposition*, Journal of Computational and Applied Mathematics, 2006, 196(2), 644–651.

[8] V. S. Erturk and S. Momani, *Solving systems of fractional differential equations using differential transform method*, Journal of Computational and Applied Mathematics, 2008, 215(1), 142–151.

[9] O. Abdulaziz, I. Hashim and S. Momani, *Solving systems of fractional differential equations by homotopy-perturbation method*, Physics Letters A, 2008, 372(4), 451–459.

[10] J. Wang, T. Z. Xu, Y. Q. Wei and J. Q. Xie, *Numerical solutions for systems of fractional order differential equations with Bernoulli wavelets*, International Journal of Computer Mathematics, 2019, 96(2), 317–336.

[11] Y. Chen, X. Ke and Y. Wei, *Numerical algorithm to solve a system of nonlinear fractional differential equations based on wavelets method and the error analysis*, Applied Mathematics and Computation, 2015, 251, 475–488.

[12] M. Kumar and S. Pandit, *Wavelet transform and wavelet based numerical methods: an introduction*, International Journal of Nonlinear Science, 2012, 13(3), 325–345.

[13] F. Zhou and X. Xu, *The third kind Chebyshev wavelets collocation method for solving the time-fractional convection diffusion equations with variable coefficients*, Applied Mathematics and Computation, 2016, 280, 11–29.

[14] S. Dhawan, J. A. T. Machado, D. W. Brzeziski and M. S. Osman, *A Chebyshev wavelet collocation method for some types of differential problems*, Symmetry, 2021, 13(4), 536.

[15] M. Faheem, A. Raza and A. Khan, *Collocation methods based on Gegenbauer and Bernoulli wavelets for solving neutral delay differential equations*, Mathematics and Computers in Simulation, 2021, 180, 72–92.

[16] S. Kumbinarasaiah and K. R. Raghunatha, *The applications of Hermite wavelet method to nonlinear differential equations arising in heat transfer*, International Journal of Thermofluids, 2021, 9, 100066.

[17] J. Shahni and R. Singh, *Laguerre wavelet method for solving Thomas?Fermi type equations*, Engineering with Computers, 2022, 38(4), 2925–2935.

[18] S. Erman, A. Demir and E. Ozbilge, *Solving inverse nonlinear fractional differential equations by generalized Chelyshkov wavelets*, Alexandria Engineering Journal, 66, 2023, 947–956.

[19] X. Li, *Numerical solution of fractional differential equations using cubic B-spline wavelet collocation method*, Communications in Nonlinear Science and Numerical Simulation, 2012, 17(10), 3934–3946.

[20] G. Manohara and S. Kumbinarasaiah, *Numerical approximation of the typhoid disease model via Genocchi wavelet collocation method*, Journal of Umm Al-Qura University for Applied Sciences, 2024, 1–16.

[21] T, N. Vo, M. Razzaghi and P. T. Toan, *Fractional-order generalized Taylor wavelet method for systems of nonlinear fractional differential equations with application to human respiratory syncytial virus infection*, Soft Computing, 2022, 26, 165–173.

[22] G. Manohara and S. Kumbinarasaiah, *Numerical solution of some stiff systems arising in chemistry via Taylor wavelet collocation method*, Journal of Mathematical Chemistry, 2024, 62(1), 24–61.

[23] J. Xie, T. Wang, Z. Ren, J. hang and L. Quan, *Haar wavelet method for approximating the solution of a coupled system of fractional-order integral?differential equations*, Mathematics and Computers in Simulation, 2019, 163, 80–89.

[24] F. Li, H. M. Baskonus, S. Kumbinarasaiah, G. Manohara, W. Gao and E. Ilhan, *An efficient numerical scheme for biological models in the frame of Bernoulli wavelets*, Comput Model Eng Sci, 2023, 137(3).

[25] K. Srinivasa, H. M. Baskonus and Y. Guerrero Sánchez, *Numerical solutions of the mathematical models on the digestive system and covid-19 pandemic by hermite wavelet technique*, Symmetry, 2021, 13(12), 2428.

[26] S. Kumbinarasaiah, *Hermite wavelets approach for the multi-term fractional differential equations*, Journal of Interdisciplinary Mathematics, 2021, 24(5), 1241–1262.

[27] Y. Chen, X. Ke and Y. Wei, *Numerical algorithm to solve system of nonlinear fractional differential equations based on wavelets method and the error analysis*, Applied Mathematics and Computation, 2015, 251, 475–488.

[28] A. Secer and S. Altun, *A new operational matrix of fractional derivatives to solve systems of fractional differential equations via legendre wavelets*, Mathematics, 2018, 6(11), 238.

[29] F. Mohammadi and C. Cattani, *A generalized fractional-order Legendre wavelet Tau method for solving fractional differential equations*, Journal of Computational and Applied Mathematics, 2018, 339, 306–316.

[30] L. I. Yuanlu, *Solving a nonlinear fractional differential equation using Chebyshev wavelets*, Communications in Nonlinear Science and Numerical Simulation, 2010, 15(9), 2284–2292.

[31] M. ur Rehman and U. Saeed, *Gegenbauer wavelets operational matrix method for fractional differential equations*, Journal of the Korean Mathematical Society, 2015, 52(5), 1069–1096.

[32] M. Mulimani and K. Srinivasa, *A novel approach for Benjamin-Bona-Mahony equation via ultraspherical wavelets collocation method*, International Journal of Mathematics and Computer in Engineering, 2024, 2(2), 179–192.

[33] G. Manohara and S. Kumbinarasaiah, *Fibonacci wavelet collocation method for the numerical approximation of fractional order Brusselator chemical model*, Journal of Mathematical Chemistry, 2023, 1–31.

[34] F. A. Shah, M. Irfan, K. S. Nisar, R. T. Matoog and E. E. Mahmoud, *Fibonacci wavelet method for solving time-fractional telegraph equations with Dirichlet boundary conditions*, Results in Physics, 2021, 24, 104123.

[35] H. M. Srivastava, M. Irfan and F. A. Shah, *A Fibonacci wavelet method for solving dual-phase-lag heat transfer model in multi-layer skin tissue during hyperthermia treatment*, Energies, 2021, 14(8), 2254.

[36] S. Sabermahani, Y. Ordokhani and S. A. Yousefi, *Fibonacci wavelets and their applications for solving two classes of time varying delay problems*, Optimal Control Applications and Methods, 2020, 41(2), 395–416.

[37] G. Manohara and S. Kumbinarasaiah, *An innovative Fibonacci wavelet collocation method for the numerical approximation of Emden-Fowler equations*, Applied Numerical Mathematics, 2024, 201, 347–369.

[38] N. A. Nayied, F. A. Shah and M. A. Khanday, *Fibonacci Wavelet Method for the Numerical Solution of Nonlinear Reaction-Diffusion Equations of Fisher-Type*, Journal of Mathematics, 2023.

[39] M. Kumar and K. N. Rai, *Numerical simulation of time-fractional bioheat transfer model during cryosurgical treatment of skin cancer*, Computational Thermal Sciences: An International Journal, 2021, 13(4).

[40] S. Shiralashetti and L. Lamani, *A modern approach for solving nonlinear Volterra integral equations using Fibonacci wavelets*, Electronic Journal of Mathematical Analysis and Applications, 2021, 9(2), 88–98.

[41] G. Manohara and S. Kumbinarasaiah, *Numerical approximation of fractional SEIR epidemic model of measles and smoking model by using Fibonacci wavelets operational matrix approach*, Mathematics and Computers in Simulation, 2024, 221, 358–396.

[42] W. M. Abd-Elhameed and Y. H. Youssri, *A novel operational matrix of Caputo fractional derivatives of Fibonacci polynomials: Spectral solutions of fractional differential equations*, Entropy, 2016, 18(10), 345.

[43] H. M. Srivastava, F. A. Shah and N. A. Nayied, *Fibonacci Wavelet Method for the Solution of the Non-Linear Hunter?Saxton Equation*, Applied Sciences, 2022, 12(15), 7738.

[44] S. C. Shiralashetti and L. Lamani, *Fibonacci wavelet based numerical method for the solution of nonlinear Stratonovich Volterra integral equations*, Scientific African, 2020, 10:e00594.

[45] S. Kumbinarasaiah, G. Manohara and G. Hariharan, *Bernoulli wavelets functional matrix technique for a system of nonlinear singular Lane Emden equations*, Mathematics and Computers in Simulation, 2022, 204, 133–165.

[46] K. Srinivasa and R. A. Mundewadi, *Wavelets approach for the solution of nonlinear variable delay differential equations*, International Journal of Mathematics and Computer in Engineering, 2023, 1(2), 139–148.

[47] Y. Ozturk, *Numerical solution of systems of differential equations using operational matrix method with Chebyshev polynomials*, Journal of Taibah University for Science, 2018, 12(2), 155–162.